Final Degree Project

Biomedical Engineernig Degree

Development of a Temperature-Controlled Environment for Neurovalidation

Barcelona, 11th June 2025

Author: Guillermo Mora

Director/s: Neri Ruiz, Jordi Colomer

Tutor: Jordi Colomer

I would like to express my deepest gratitude to all those who have supported and guided me throughout the development of this Final Degree Project.

First and foremost, I would like to thank my tutor and member, Dr. Jordi Colomer, for his continuous support, guidance, and trust during every stage of the project. His expertise, patience, and critical insight were fundamental in shaping this work and helping me overcome the many technical and conceptual challenges encountered along the way. I would also like to thank the members of the ThermoNOoC Project (PID2022-137190OB-I00), funded by the Ministry of Science, Innovation and Universities, for allowing me to participate and contribute to the project.

I am also sincerely grateful to the project's director Neri Ruiz, who shared her knowledge on electronics, Arduino Uno, and LabView, making a significant difference in the successful implementation of the system. From helping with equipment setup to troubleshooting unexpected problems, your collaboration was invaluable.

Finally, I would like to thank all the people who, in one way or another, contributed to this project through encouragement, shared knowledge, or simply by offering their support when it was most needed.

To all of you, thank you for being a part of this journey.

Abstract

This Final Degree Project presents the design and implementation of a temperature-controlled chamber for studying the behavior of neural precursors under varying thermal conditions. The chamber is intended as a core component within a broader initiative aimed at developing non-invasive therapeutic devices for epilepsy treatment, particularly through ultrasound-induced brain cooling.The device enables precise environmental temperature control. Its design integrates heating elements, high-precision digital temperature sensors (TSIC 506F), and a closed-loop control system managed by an Arduino Uno microcontroller, as well as a LabVIEW-based interface developed for real-time data visualization and logging.

A methacrylate structure, supported by 3D-printed components, was selected for its transparency and ease of fabrication after multiple versions were investigated to optimize chamber structure, thermal distribution, and sensor integration. Both passive and forced-convection heating methods were analyzed, with thermal validation conducted using infrared imaging. The chamber consistently achieved the desired thermal range (36–37.5 °C), demonstrating spatial uniformity in controlled experiments and representing an initial platform for analyzing the impact of temperature on neural activity, contributing valuable data for the design of future brain-cooling neuromodulation devices.

Keywords: Neuroengineering, Temperature control, Neural precursors, Epilepsy, Brain cooling, Arduino, LabVIEW, Thermal chamber, Biomedical engineering, Ultrasound neuromodulation

Abstract

Aquest Treball de Fi de Grau presenta el disseny i la implementació d'una cambra amb control de temperatura per estudiar el comportament dels precursors neuronals sota condicions tèrmiques variables. La cambra està concebuda com un component clau dins d'una iniciativa més àmplia orientada al desenvolupament de dispositius terapèutics no invasius per al tractament de l'epilèpsia, especialment mitjançant el refredament cerebral induït per ultrasons.

El dispositiu permet un control precís de la temperatura ambiental ja que el seu disseny integra elements calefactors, sensors de temperatura digitals d'alta precisió (TSIC 506F) i un sistema de control en bucle tancat gestionat per un microcontrolador Arduino Uno, així com una interfície basada en LabVIEW per a la visualització i registre de dades en temps real.

S'han explorat diverses versions per optimitzar l'estructura de la cambra, la distribució tèrmica i la integració dels sensors: es va escollir una estructura de metacrilat per la seva transparència i facilitat de fabricació, reforçada amb elements impresos en 3D. Es van analitzar mètodes de calefacció passiva i per convecció forçada, i es va dur a terme una validació tèrmica mitjançant imatges infraroges. La cambra va assolir de manera consistent el rang tèrmic desitjat (36–37,5 °C), demostrant una uniformitat espacial en experiments controlats i representant una plataforma inicial per analitzar l'impacte de la temperatura sobre l'activitat neural, aportant dades valuoses per al disseny de futurs dispositius de neuromodulació per refredament cerebral.

Paraules clau: Neuroenginyeria, Control de temperatura, Precursors neuronals, Epilèpsia, Refredament cerebral, Arduino, LabVIEW, Cambra tèrmica, Enginyeria biomèdica, Neuromodulació per ultrasons.

Content

1. Introduction

1.1 Objectives

The use of technology in medicine has been growing over time, helping improve disease prevention and treatment. As a result, a proposal was made to use technology to treat epilepsy. Millions of people worldwide have epilepsy, a chronic neurological disorder. Even with advances in medical care and knowledge, a significant portion of patients still suffer seizures, which can severely impact their quality of life. Ultrasound neuromodulation is a promising study area with the potential to transform epilepsy treatment through new, less intrusive approaches. Ultrasound-based neuromodulation offers the promise of a focused, less intrusive therapy compared to conventional treatments like brain surgery or deep brain stimulation. Modulating neural activity by generating cold spots provides a unique approach for controlling epileptic seizures.

Brain cooling, known in medicine as therapeutic hypothermia, is one of the most promising strategies in this field. This technique involves reducing the patient’s body temperature and has shown beneficial effects in several medical areas, especially in treating acute brain injuries such as strokes and traumatic brain injuries. In this context, temperature is a critical factor for brain activity and the optimal functioning of the nervous system.

This final degree project is part of a larger initiative: designing and developing an ultrasound neuromodulation device, intended to be implanted in the brain and act on the affected area in patients with this condition. The device's innovative operation will allow for the controlled generation of cold spots via ultrasound, enabling the reduction of temperature in the neural area responsible for seizures during an epileptic episode.

More specifically, this project aims to contribute to developing such a device by designing and building a container capable of maintaining desired temperature conditions to study neural precursors inside it. The goal is to monitor and quantify the relationship between environmental temperature and neural activity. This container will allow for the observation of neural cells using thermal cameras and/or microscopes, facilitating the analysis of their behavior in controlled conditions, through the implementation of an observation system capable of continuously and precisely recording the activity of neural precursors inside the container. The system may also include high-resolution cameras for capturing detailed images and videos that, together with thermal cameras, will allow for effective monitoring of the relationship between temperature and the electrical activity of the precursors. This is the main objective of the project.

The project seeks to advance the field of neuromodulation and provide a solid foundation for exploring new therapeutic approaches that could significantly improve the quality of life for people with epilepsy. This research aims to push healthcare toward a future where epilepsy becomes more manageable and less intrusive for those affected.

1.2 Scope of the Project

The project involves designing, developing, and implementing a device to monitor the electrical activity of neural precursors in response to the temperature of their environment. This includes the creation of a transparent container, integrating an observation system with cameras and/or microscopes, incorporating temperature sensors, and establishing experimental protocols to record and analyze the electrical data of the precursors.

It is important to emphasize that this project is a small part of a larger initiative developed by the University of Barcelona thanks to the ThermoNOoC Project (PID2022-137190OB-I00) founded by the '*Ministerio de Ciencia, Innovación y Universidades'*, to develop innovative brain devices to treat epilepsy.

Within this context, the design and development of the monitoring device for neural precursor electrical activity, carried out at the University of Barcelona, is a foundational piece of this larger project. This device plays a crucial role in providing fundamental information about the electrical activity of neural cells and their relationship with brain temperature, which is essential for designing and optimizing ultrasonic cooling devices.

In summary, this project is conceived as an essential part of a larger puzzle whose goal is the development of innovative brain devices for treating epilepsy. Each component and each step forward, including the monitoring device designed in this work, contributes to improving the quality of life of people affected by epilepsy by developing more effective therapeutic solutions.

2. Background

2.1 State of the Art of the Technology

The current state of brain device technology for treating epilepsy is an active research and development phase. Although various technologies and approaches exist for epilepsy treatment, ultrasound for brain cooling is emerging as a promising and relatively new area.

Several studies have demonstrated the effectiveness of brain cooling through ultrasound in reducing neuronal activity and preventing epileptic seizures. For instance, research by Lee et al. (2018) [1] explored using ultrasound to modulate brain activity and control epilepsy in animal models. This study provides initial evidence supporting the feasibility of this technique as a therapeutic strategy for epilepsy.

Moreover, devices in neuroscience and biomedical engineering are being developed to monitor neuronal activity in real time. These devices allow the recording and analysis of the electrical activity of neural cells in response to different stimuli and environmental conditions. Research by Jun et al. (2017) [2] presents advances in developing high-resolution, high-precision brain activity recording systems.

In the specific context of this project—monitoring the electrical activity of neural precursors in response to environmental temperature—there is a need for specialized devices that allow for a detailed and precise study of this relationship. While established techniques exist for recording neuronal electrical activity, integrating monitoring with real-time temperature measurement is a less explored area that requires the development of specific devices.

2.2 Current Situation

Currently, various methods and therapies have been studied to prevent or reduce the effects of epileptic seizures from three main approaches: medication, brain stimulation, and transplantation of the brain cells responsible for the seizures.

Regarding the first approach, in recent years, several new anti-seizure medications (ASMs) have been developed and proven effective for treating different types of epilepsy. Among them are Brivaracetam, a derivative of Levetiracetam with high affinity for the synaptic vesicle protein 2A, showing efficacy in focal epilepsy [3]; and Cannabidiol (CBD), approved for the treatment of rare syndromes such as Dravet and Lennox-Gastaut, which acts via similar mechanisms.

In brain stimulation, the main treatments include Vagus Nerve Stimulation (VNS), which involves implanting a device that sends electrical pulses to the vagus nerve to help reduce seizure frequency and severity. Deep Brain Stimulation (DBS) consists of the implantation of electrodes in specific brain areas, such as the anterior nucleus of the thalamus, to modify brain activity and prevent seizures [4].

Finally, there is Responsive Neurostimulation (RNS), a technique that detects brain activity patterns that precede a seizure and delivers immediate electrical stimulation to interrupt it [5].

Lastly, one of the primary approaches includes brain cell transplantation, which aims to restore the balance between excitation and inhibition in the brain by transplanting cells that release inhibitory neurotransmitters such as GABA. Preclinical studies have shown that this method can reduce the frequency and severity of epileptic seizures without the need to remove brain tissue, representing a significant advancement over traditional surgical techniques [6].

This analysis shows that despite ongoing research, there are currently no implantable devices available to control this type of seizure, highlighting a promising future for developing and constructing the proposed project.

3. Market Analysis

The potential of thermoelectric generators in medicine has attracted significant attention, although it has not been fully explored. Various studies and articles highlight that thermoelectric generators uniquely convert heat into electrical energy, whether generated by the human body or by external heat sources, thus providing an efficient power source without relying on basic electronic components. Different studies and experiments related to thermoelectric generators and brain implants have been considered for the development of the device.

One study by researchers at the Public University of North Carolina developed an innovative method to convert body heat into electricity more efficiently than current systems. This new system is compact, lightweight, and flexible, with dimensions of one square centimeter and two millimeters thick, and it can produce up to 20 microwatts per square centimeter. It is based on a conductive layer that collects body heat and concentrates it on a thermoelectric generator. At the same time, an outer polymer reduces heat loss before it passes through the generator. This design can be integrated into clothing or placed directly on the body, preferably on the upper arm. Despite its limited electrical output, it is expected to power health and environmental sensors, such as heart rate monitors or air quality sensors [7].

Research has also been conducted on developing a wearable known as the Matrix PowerWatch wristband, which uses body heat as its energy source. By harnessing the temperature of the wrist, it acts as a heat sink that transfers heat to the thermoelectric generator located at the top of the watch face, thus generating the necessary electricity. Due to its limited power, the watch features a low-power electronic ink display and basic functions such as physical activity tracking and syncing with mobile devices. It enters a sleep mode to minimize energy consumption when not in use. Although it is not yet commercially available, it could represent a significant breakthrough for wearable devices by eliminating the need to recharge batteries [7].

Significant progress has been made in the brain-computer interface (BCI) field, particularly by Neuralink, a company founded by Elon Musk. To treat complex neurological conditions and improve patients' quality of life, Neuralink successfully performed its first brain chip implant in a human [8]. The procedure involves inserting a tiny, fully sealed chip into the patient's brain. This chip connects to 1,024 ultra-thin electrodes and operates through a rechargeable battery without wires. The created interface enables bidirectional communication with an external computer, facilitating the sending and receiving of signals.

The patient may gain complete control of a computer mouse, play chess, and play music solely through direct brain signals. This advancement demonstrates the transformative potential of BCIs in improving the quality of life and autonomy.

However, this technology presents several risks and concerns. In the short term, any brain surgery carries inherent physical risks. Given the brain's complexity and the lack of data on the long-term effects of having an implanted device, the medical implications remain uncertain [8]. Furthermore, ethical issues arise regarding data protection, potential abuse, and the development of enhanced human cognitive capabilities.

While Neuralink has made great strides with its first human brain implant, a similar breakthrough was achieved by a research team led by neuroscientist Grégoire Courtine from the Swiss Federal Institute of Technology (EPFL) and neurosurgeon Jocelyne Bloch from the University Hospital of Vaud in Switzerland. They significantly improved mobility in individuals with spinal cord injuries [10].

Using wireless technology, two electronic devices were digitally connected. According to Bloch, electrodes were inserted into the brain region responsible for leg movement. These electrodes can decode brain signals related to walking. Additionally, a neurostimulator connected to a set of spinal electrodes was implanted. This enables stimulation of leg muscles, provoking the desired movement. Thanks to this technology, the patient can move freely again. Considering the significance of these advances, a project published in JAMA Neurology has investigated a potential treatment for epilepsy using a focal cooling system [9].

Drug-resistant epilepsy (DRE) remains a major clinical challenge. Although surgery may be an option for some patients, it has limitations such as irreversibility, restricted brain areas, and limited accessibility. In this context, focal cooling is a feasible and promising solution. This method has been proven safe and effective through animal and human studies, as it is reversible and does not rely on medications.

First, scientific studies demonstrating the efficacy and safety of focal cooling for treating DRE are analyzed. Then, its potential development as an innovative therapeutic option for affected patients is presented. Seizure control has been effectively achieved by intraoperative application of cold saline to a specific area. Although the exact mechanism is not fully understood, research indicates that it decreases synaptic activity by reducing neurotransmitter release and altering dendritic spine structures. Moreover, focal cooling reduces neuronal activity and modulates seizure thresholds and membrane channel functions at the cellular level.

4. Conceptual Engineering

4.1 Theoretical Background

The foundations of this project are based on the accurate generation of heat through the Joule effect using heating resistors and fans, as well as the precise reading and monitoring of temperature values by sensors placed inside the device. For this reason, these two principles must be precisely defined and implemented to ensure optimal conditions for conducting subsequent studies.

The Joule Effect

The Joule effect is a fundamental physical phenomenon that describes converting electrical energy into thermal energy when an electric current passes through a conductor with electrical resistance. This process occurs due to collisions between the free-moving electrons and the fixed ions in the resistive material, transferring kinetic energy into thermal energy [11]. These microscopic interactions cause the material's temperature to rise.

The amount of heat *'Q'* generated by a resistive element is given by the equation:

$$Q = I^2 \cdot R \cdot t$$

Equation 1.- Equation describing the Joule Effect, where Q is the heat produced (in joules), I is the current (in amperes), R is the resistance (in ohms), and t is the time (in seconds).

Where Q is the heat generated (in joules), I is the electric current (in amperes), R is the resistance of the conductor (in ohms), and t is the time during which current flows (in seconds).

This relationship illustrates that the thermal energy produced is directly proportional to the square of the current, the resistance, and the conduction time. In practical applications, such as in this project, Joule heating is used to control the internal temperature of a chamber by powering resistive heating elements with a regulated electric current.

On the other hand, temperature sensors convert thermal energy into readable electrical signals that electronic control systems can interpret. In general, temperature sensing can be based on various physical principles, including [12]:

- **Resistance change** (e.g., RTDs and thermistors),
- **Thermoelectric voltage generation** (e.g., thermocouples),
- **Semiconductor behavior** (e.g., integrated temperature sensors like the TMP36).

The output of such sensors is typically a voltage, resistance, or current that varies predictably with temperature. These outputs can then be digitized and used in feedback control systems to regulate heating or cooling mechanisms.

TMP36 Temperature Sensor: Voltage-to-Temperature Conversion

The TMP36 [16] is a low-voltage precision analog temperature sensor that provides a linear voltage output directly proportional to temperature. It is factory-calibrated and does not require additional components, making it ideal for microcontroller-based systems [13].

The TMP36 has the following characteristics:

- Output voltage of 750 mV at 25 °C,
- A scale factor of 10 mV/°C,
- An offset of 500 mV at 0 °C,
- Operating voltage range: 2.7V – 5.5V,
- Accuracy of ±2 ° to cover typical temperature ranges.

The temperature can be calculated from the sensor's output voltage using the equation:

$$T(°C) = \frac{V_{out} - 500mV}{10\ mV/°C}$$

Equation 2.- Equation describing the reading temperature from the TMP36 sensors

Where V_{out} is the sensor's output voltage in millivolts.

In systems such as this project, the output voltage is read through an analog input pin of a microcontroller (e.g., Arduino), which provides a digital value from 0 to 1023 based on a reference voltage (usually 5V). The analog reading is converted to voltage with:

$$V_{out} = \frac{analogRead \cdot V_{ref}}{1023}$$

Equation 3.- Equation describing the conversion between Arduino's analog read and the output voltage

Once the voltage is known, the temperature can be accurately determined using the TMP36 conversion formula. This measurement is essential for implementing closed-loop thermal control, where heating or cooling components are activated in response to real-time temperature changes.

4.2 Hardware Design

4.2.1 Methacrylate and Microcontroller’s Chamber

Various options and methodologies must be considered when designing and constructing a device to monitor the relationship between the electrical activity of neural precursors and the temperature of their environment. The goal is to select the best solution that meets the project requirements and facilitates the collection of accurate and valuable results.

There are several approaches to the design and development of the device. One of the most viable options is the design of a single container with unified temperature control, which simplifies the system’s design and construction by enabling uniform environmental control and facilitating observation. However, this option does not allow studying electrical activity variability in response to temperature differences within the same container.

Another option is to divide the container into two thermally insulated sections, each with its temperature control. This approach allows for comparing neural precursor activity under different thermal conditions within a single experiment. Nevertheless, it increases the complexity of the design and construction and requires a more advanced thermal insulation and control system.

A third option involves creating a rectangular container with thermal plates at both ends, generating a temperature gradient from one side to the other. This design enables continuous analysis of electrical activity across a range of temperatures, making it easier to identify optimal and critical points of neural activity. Although it requires precise control of the temperature gradient and greater data measurement and recording accuracy, this option offers the most significant advantages for the project's goals.

Finally, a modular system is proposed, consisting of several small containers connected in series or parallel, each with its own temperature control. This modular configuration allows multiple experiments to be carried out simultaneously under controlled and comparable conditions. Modularity also facilitates the repair and replacement of individual components without affecting the entire system, although it increases the complexity of assembly and calibration of each module.

Despite the differences in design, all of these share a common feature: 3D modeling using platforms such as FreeCAD [15] or similar software for subsequent printing and cutting on acrylic (PMMA) sheets, as it is the most cost-efficient solution to develop this project successfully. However, it is essential to note that acrylic (PMMA) is not inherently biocompatible for cell culture, as its smooth and non-porous surface can hinder cell adhesion. To address this limitation, surface treatments can be applied to improve its biocompatibility. These may include coatings with extracellular matrix proteins such as collagen, laminin, or poly-L-lysine, which promote cell adhesion and growth. Another effective method is plasma treatment, which introduces functional groups onto the surface to enhance cell attachment. While this technique is more complex, it can be highly effective. Alternatively, materials such as treated glass or polystyrene can be used, as they are often pre-coated with biocompatible substances to support cell adhesion and proliferation.

Suppose acrylic is to be used without any surface modification. In that case, another viable option is to place standard culture devices within the container that support the growth of neural precursors, such as Petri dishes, and then apply the temperature gradient through thermally conductive fluid (either liquid or gas). The feasibility of each approach should be evaluated empirically, once the ability of acrylic to contain neural precursors and their medium has been tested in practice. The most appropriate path forward can be determined based on the results.

To carry out the 3D design of the container, the first step was to develop a representation in SketchUp [14] of a potential final model, which was then translated into 3D design software using a file format suitable for later cutting on the acrylic sheet. This initial representation allowed the visualization of a possible final design, which served as a basis for further development. From there, work began constructing the acrylic chamber by creating and refining several design iterations.

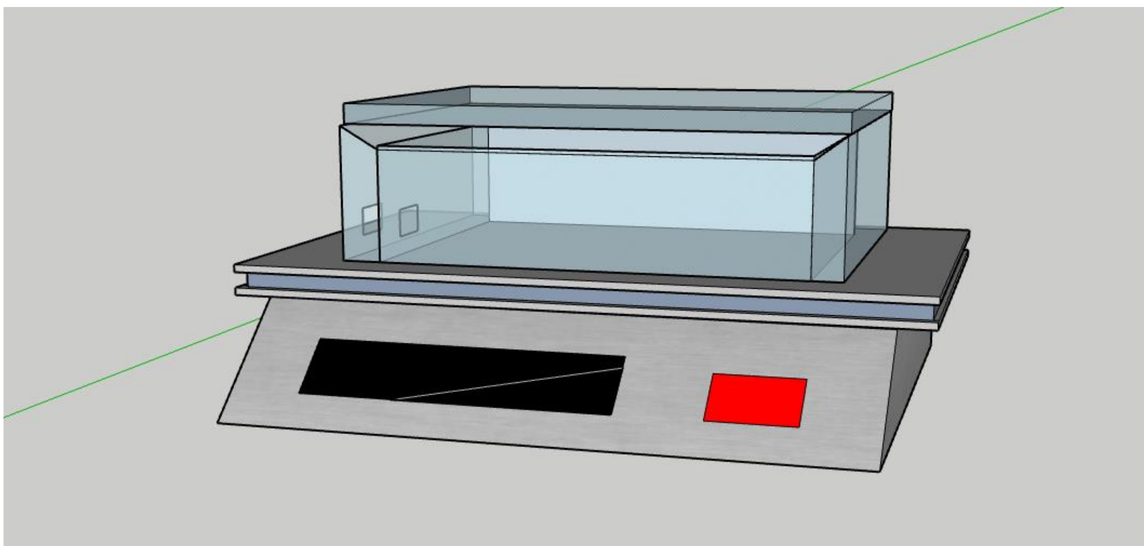

Figure 1.- Image of the initial 3D design using SketchUp software

When planning the 3D designs, it was essential to evaluate and compare different methods for joining the chamber components to ensure a leak-free structure and avoid any damage to the acrylic. Two alternatives were ultimately considered. The first, a more straightforward approach, involved assembling the chamber components using screws. The second, with a more complex design, proposed creating interlocking pieces to be later joined using a specific acrylic adhesive that would guarantee the robustness and stability of the structure. All proposed designs were developed with the same measures: 300x210x150 mm.

4.2.2 Heating Elements

Since the beginning of the project, the plan was to use multiple heating elements to ensure either uniform or a temperature gradient inside the chamber. Among the options considered throughout the project, the most basic component, which has remained unchanged since the beginning, was using a set of heating resistors.

Heating resistors are electrical components specifically designed to convert electrical energy into heat through the Joule effect. When an electric current flows through a resistive material, the electrons collide with the atoms in the conductor, producing vibrations that generate thermal energy. This process is described by the Joule heating equation [Equation 1]. In the context of this project, heating resistors provide a controlled and localized heat source to adjust the temperature within the chamber; their simplicity, reliability, and precise thermal response make them an ideal choice for maintaining the necessary thermal conditions for biological experimentation.

Amongst the large variety of heating resistors available in the market, one of the main options was a self-regulating Positive Temperature Coefficient (PTC) heater from the ΩDBK HPG Series [17] to achieve precise thermal control within the experimental chamber. These heaters are designed for both AC and DC applications, operating within a voltage range of 100–240V and offering surface temperatures selectable from 40 °C to 240 °C in 10 °C increments (±7 °C). Their compact and robust design—typically 40 x 35 mm with silicone-insulated AWG20 lead wires—facilitates integration into limited spaces, making them particularly suitable for biomedical setups.

A key advantage of the HPG Series lies in its self-regulating nature. As the surface temperature rises, the internal resistance increases, reducing current flow and stabilizing the temperature without requiring external thermal controllers. This intrinsic safety mechanism minimizes the risk of overheating and enhances system reliability. Moreover, the heater's compliance with RoHS directives [18] and Protection Class II [19] standards supports safe and environmentally responsible usage. Despite these benefits, several limitations must be acknowledged. The fixed surface temperature settings may constrain the flexibility needed for fine-tuned thermal experiments. Additionally, the heater exhibits an initial inrush current at startup, which must be managed within the power design. Finally, while the heater surface reaches the set temperature reliably, supplementary mechanisms may be required to ensure uniform temperature distribution across the entire volume of the chamber.

In addition to the previously discussed self-regulating PTC heater, the project initially considered integrating forced convection heaters to ensure uniform temperature distribution within the experimental chamber. Two specific models from DBK Enclosures were evaluated: the FGC0501.2 [20] and the FGC1507.2 [21].

The FGC0501.2 is a compact fan heater operating at 12 V DC with a power output of 20 W and a surface temperature of approximately 35 °C. Its integrated axial fan facilitates the circulation of warm air, promoting even heat distribution. This model's low power consumption and compact design make it suitable for small-scale applications where precise temperature control is essential. Conversely, the FGC1507.2 is a more robust unit designed for larger enclosures. It operates within a 100–240 V AC voltage range, delivering a power output of 230 W and achieving a surface temperature of up to 120 °C. The integrated fan provides an airflow of 12.4 m^3/h, ensuring rapid and uniform heating across the chamber, making it particularly advantageous for applications requiring swift temperature stabilization over a broader area.

While both heaters offer self-regulating capabilities and integrated fans for uniform heat distribution, their selection depends on the specific requirements of the experimental setup, including chamber size, desired temperature range, and available power sources. The FGC0501.2 is ideal for precise, low-power applications, whereas the FGC1507.2 suits scenarios demanding higher power and rapid temperature stabilization.

4.2.3 Temperature sensors

In developing the temperature-controlled chamber, two temperature sensors were considered: the TMP36 by Analog Devices [16] and the TSic 506F by IST AG [22]. Both are integrated temperature sensors designed for microcontrollers but differ significantly in output type, accuracy, and power consumption.

The TMP36 is an analog sensor known for its simplicity and ease of integration. It provides a linear voltage output of 10 mV/°C, with an offset of 500 mV at 0 °C and a typical output of 750 mV at 25 °C. It operates within a temperature range of –40 °C to +125 °C and offers acceptable accuracy for many general-purpose applications, with a typical error of ±2 °C at room temperature. Due to its analog nature, it is susceptible to electrical noise and resolution limits from the analog-to-digital converter used in the system.

In contrast, the TSic 506F is a digital temperature sensor that communicates via the ZACWire [23] protocol and offers a much higher precision, with an accuracy of ±0.1 °C in the +5 °C to +45 °C range. This sensor is fully calibrated at the factory and provides excellent long-term stability, making it ideal for applications where reliability and accuracy are critical. It operates at a low supply current (typically 30 µA at 3.3 V), which helps minimize self-heating, and is suitable for low-power environments. However, its narrower temperature range (–10 °C to +60 °C) and the need for a digital decoding interface add complexity to its integration.

Overall, while the TMP36 offers an affordable and straightforward solution for basic temperature monitoring, the TSic 506F stands out for its precision and digital stability, making it the preferred choice for applications that require high accuracy and low power consumption.

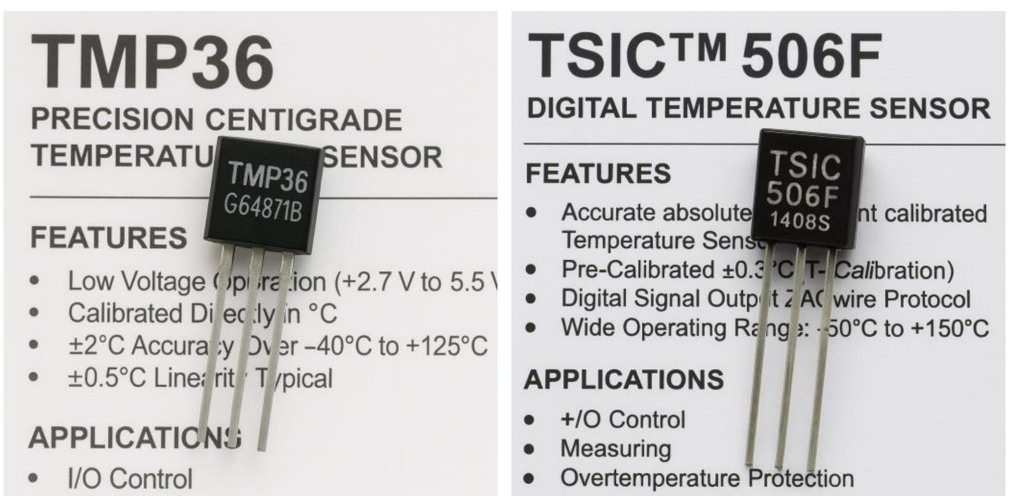

Figure 2.- Image of the TMP36 [16] and TSIC 506F [22] temperature sensors. AI generated.

4.2.4 Microcontroller selection: Arduino Uno

The Arduino Uno [24] is an open-source microcontroller board based on the ATmega328P. It operates at 5 V with a recommended input voltage of 7–12 V and provides a maximum DC of 40 mA per I/O pin. The board features 14 digital input/output pins (6 of which can be used as PWM outputs), six analog inputs with a 10-bit resolution ADC, 32 KB of flash memory (0.5 KB used by the bootloader), 2 KB of SRAM, and 1 KB of EEPROM. Physically, the board measures 68.6 mm × 53.4 mm and includes a USB port for programming and serial communication.

In this project, the Arduino Uno is the central unit for reading temperature values from analog sensors like the TMP36 and decoding digital signals from the TSic 506F. Its analog inputs allow direct voltage readings from the TMP36 without external components, while its digital pins, combined with custom timing routines, can decode the ZACWire protocol from the TSic sensor. Furthermore, PWM outputs can drive solid-state relays or control signals for self-regulating PTC heaters. These temperature sensors can be interfaced with the board's analog and digital pins. The TMP36 provides a voltage output that varies linearly with temperature, which is read through one of the Arduino's analog inputs using the built-in 10-bit ADC (Analog-to-Digital Converter). The ADC converts this voltage to a digital value, which can be interpreted in degrees Celsius using a simple linear formula [Equation 2].

In contrast, the TSic 506F communicates via a digital protocol (ZACWire). This requires the Arduino to read the timing of a single-wire digital signal using precise interrupt-based or time-sensitive code to decode the temperature value transmitted by the sensor.

Once the temperature is acquired, the Arduino processes the data and compares it against a predefined setpoint. If the measured temperature is below the target range, the Arduino activates a heating element using a relay or transistor-based switch. For example, a digital output pin can be set HIGH to energize a relay module, which powers an external PTC heater connected to the mains supply. Arduino can implement simple on/off control (hysteresis-based) or more advanced logic like PWM modulation (for low-voltage heating elements) to regulate power delivery.

This closed-loop system allows the Arduino to maintain the chamber's temperature within precise limits. Additionally, real-time temperature readings and heater status can be displayed through a serial monitor or visualized on external displays, enabling the user to monitor and log performance throughout the experiment.

Data acquisition and visualization are facilitated through the serial interface or other tools, enabling real-time monitoring via a connected PC or integration with external displays such as LCD or OLED modules.

4.3 Code and Data Visualization

Several approaches were considered to implement the control logic of the thermal regulation system. The main solution chosen was to develop the code directly on the Arduino Uno using the Arduino IDE. This approach enables low-level control of sensors and actuators, allowing the microcontroller to read analog or digital temperature values and activate heating elements via digital outputs connected to relays.

The Arduino environment offers a lightweight, open-source platform with broad community support, making it ideal for rapid prototyping. Its simplicity and efficiency are significant advantages, particularly in real-time systems with limited computational needs. However, it also presents some limitations, such as reduced processing power and memory, which can constrain complex algorithms or high-frequency data acquisition. Additionally, it lacks integrated tools for advanced data analysis or graphical monitoring.

LabVIEW (Laboratory Virtual Instrument Engineering Workbench) [25] by National Instruments was selected as the preferred tool for visualizing and monitoring temperature data. LabVIEW provides a graphical programming interface that simplifies the design of custom dashboards and real-time monitoring systems. Through serial communication protocols such as VISA or LINX, it can interface directly with the Arduino to retrieve sensor data, display it graphically, and even log it for post-experiment analysis. LabVIEW's modular design, extensive library of visual components, and scalability make it especially valuable in laboratory environments. Nonetheless, its main drawbacks include the proprietary licensing model and a moderate learning curve for users unfamiliar with graphical programming. Despite this, its powerful visualization capabilities and smooth integration with Arduino hardware make it a highly effective solution for the data monitoring requirements of this project.

5. Detailed Engineering

5.1 Hardware components

5.1.1 Methacrylate Chamber and Microcontroller's Container

The methacrylate chamber [Figure 2] is constructed from flat panels designed with precision interlocking joints, facilitating modular assembly. This approach allows for secure fitting of components, enabling a rigid and stable structure essential for maintaining controlled environmental conditions during neural precursor experiments. The interlocking design distributes mechanical stress evenly and provides initial alignment and strength, simplifying the assembly process.

However, appropriate acrylic adhesives were required along the joints to achieve airtight and watertight sealing. These adhesives enhance the chamber's robustness and prevent leaks, which is critical for temperature control and to avoid contamination in biological studies. In this case, RS Pro Super Glue [26] was selected, as it provides excellent bonding strength to polymethyl methacrylate (PMMA) surfaces and creates a clear and transparent joint, preserving the optical clarity essential for the chamber's purpose. As a result, by combining mechanical interlocking and adhesive bonding, a durable and reliable enclosure was obtained, presenting different strengths and weaknesses.

The chamber's compact design optimizes internal volume while minimizing external footprint, allowing efficient integration with observation equipment such as microscopes and thermal cameras. Additionally, specific cutouts in certain panels provide dedicated access points for sensors, cables, and heating elements, facilitating organized cable management and protecting electrical connections from mechanical stress and accidental disconnection.

Utilizing methacrylate sheets leverages their excellent optical transparency, indispensable for high-resolution imaging, while their mechanical rigidity offers adequate protection for delicate samples. The flat-panel construction also streamlines fabrication processes, using laser cutting or CNC machining for cost-effective and precise manufacturing.

On the other hand, attention must be given to the limited thermal insulation properties of methacrylate and the potential constraints on expanding the chamber without redesigning panels, in addition to the proper adhesive application and maintenance, which are vital to preserving the enclosure's integrity over time.

Similarly, a 3D developed container was designed using CAD software to ensure secure storage and protection for the Arduino Uno microcontroller, relay modules, and protoboard, while facilitating efficient cable management. The structure features a robust, compact design that houses the electronic components in a dedicated space, shielding them from mechanical damage, dust, and accidental interference. Its rigid walls ensure the integrity of sensitive circuitry during handling or transportation.

The container’s open slot and cutout areas allow for easy routing and access to power lines, sensor cables, and communication interfaces without compromising the compactness of the enclosure, promoting an orderly internal layout, simplifying troubleshooting, maintenance, and potential upgrades. Moreover, the container's detachable lid facilitates quick access to the electronics for programming, modifications, or repairs, enhancing usability without requiring complete disassembly of the entire housing.

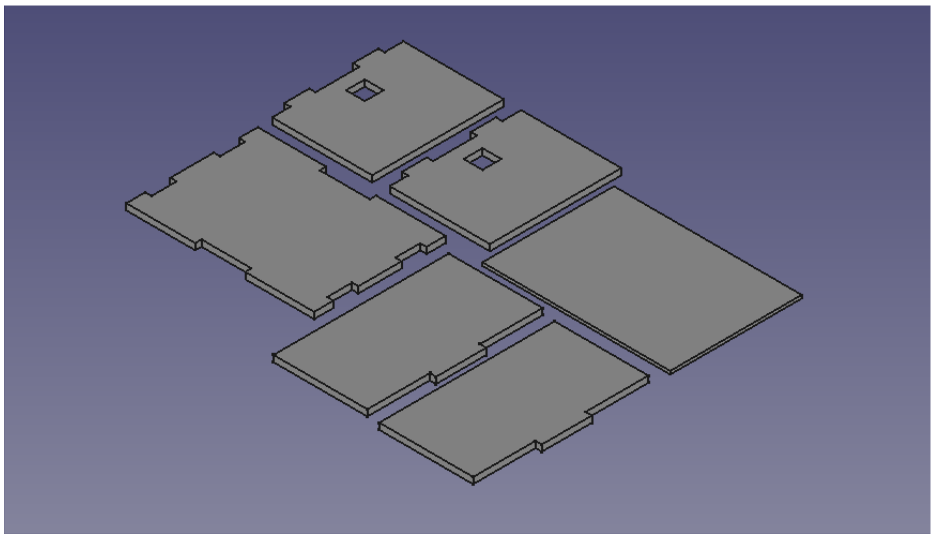

Figure 3.- Second 3D design using interlocking pieces in FreeCAD [15] 0.21.2

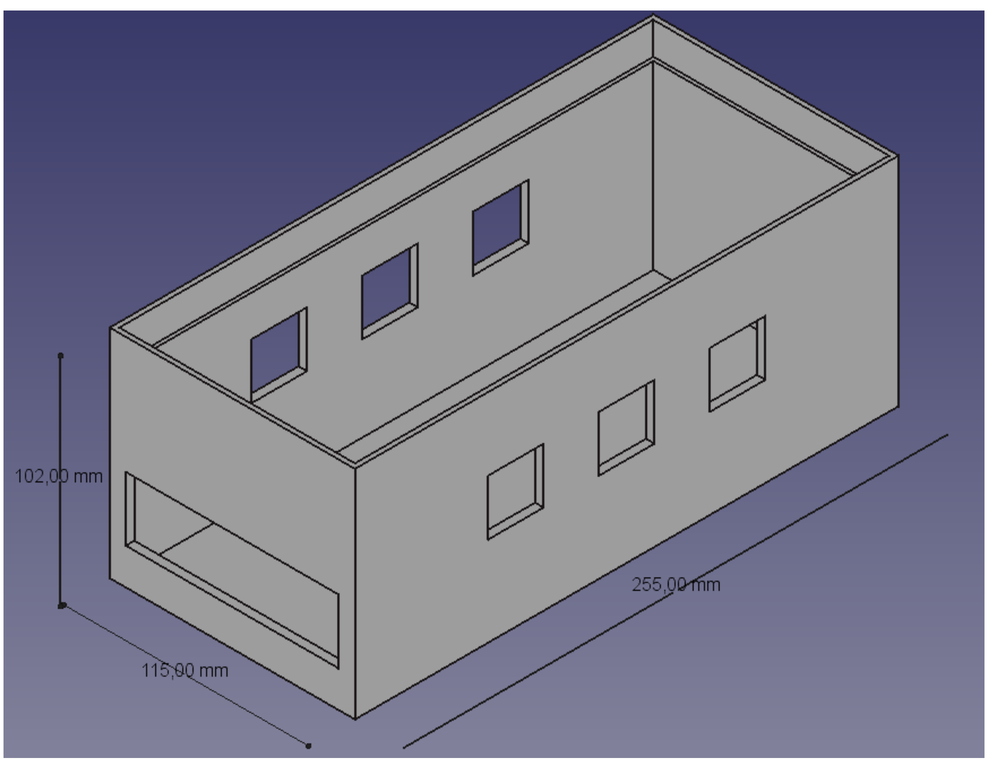

Figure 4.- Microcontroller’s container 3D design using FreeCAD [15] 0.21.2

5.1.2 Heating Elements

Heating Resistors

The ΩDBK HPG Series PTC [17] (Positive Temperature Coefficient) heating resistors are highly suitable for applications requiring safe, self-regulating, and compact thermal control, such as the temperature-controlled methacrylate chamber designed for neurovalidation experiments proposed in this project.

As explained in the conceptual engineering section, these PTC heaters are characterized by a surface temperature range selectable in 10°C increments from 40°C to 240°C (±7°C), which allows fine-tuned thermal performance across a broad range of biological and technical applications. The specific model used in this project delivers consistent heat output while automatically limiting its temperature rise, thanks to the PTC effect: as the heater warms, its internal resistance increases, reducing current flow and preventing overheating without the need for complex feedback controllers.

The compact dimensions—typically 40 mm x 35 mm—and their flat form factor allow easy integration into enclosed experimental chambers, ensuring uniform heating across a small surface area. Additionally, the silicone-insulated UL-certified [27] wiring and Class II protection rating support safe operation in a lab environment, minimizing risks of electrical hazards.

However, the PTC resistor has limitations that must be considered. Firstly, it lacks active temperature feedback or modulation, so that the heating curve may be less precise in environments with rapidly changing thermal demands. Secondly, the initial inrush current during startup can stress power supplies if not properly managed. Finally, surface heating may require additional elements, such as fans, to ensure homogeneous heat distribution within larger or irregularly shaped enclosures.

Despite these limitations, the ΩDBK HPG Series provides an efficient, low-maintenance solution for delivering steady heat in controlled environments. Its self-regulating nature, safety compliance, and ease of integration make it particularly suitable for biological research settings where temperature stability and simplicity are critical.

Two ΩDBK HPG Series PTC heating resistors were used and electrically connected in parallel through soldering to achieve consistent and distributed heating within the methacrylate chamber. This configuration ensures uniform temperature distribution across the experimental area while maintaining electrical efficiency and simplicity. The required voltage for both elements is delivered through a relay module, which serves as the intermediary between the power supply and the heater; this relay is controlled by the Arduino Uno, which executes a custom control code that monitors the internal temperature of the chamber via the TSIC 506F digital sensors. When the detected temperature falls below a predefined threshold, the Arduino activates the relay, powering the heaters. Contrarily, once the desired temperature is reached, the Arduino switches the relay off, interrupting the current flow and deactivating the heaters, ensuring stable and precise environmental conditions.

Parameter	Specification
Operating Voltage	100–240 V AC or 12–30 V AC/DC
Surface Temperature Options	40 °C to 240 °C (in 10 °C increments, ±7 °C)
Dimensions (L × W)	40 mm × 35 mm (other sizes available on request)
Leadwire	Silicone, UL 3135, AWG20, 100 ±5 mm length
Termination	6 mm splice crimp
Protection Class	Class II
Compliance	RoHS compliant
Self-Regulating	Yes (via internal PTC behavior)

Table 1. The technical specifications of the ΩDBK HPG-2/08-75X35-12-30 PTC [17] heating resistor highlight its voltage range, temperature control capabilities, and structural features relevant to controlled thermal environments.

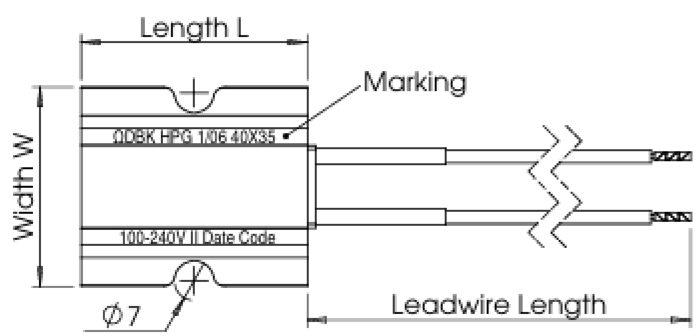

Figure 5.- Scheme of the ΩDBK HPG-2/08-75X35-12-30 PTC [17] structure

Heating Fans

To carry out this project, two DBK Cirrus 40/2 have been selected as the central heating units due to their ability to combine efficient heating with active air circulation in a compact, integrated unit. Unlike traditional resistive heaters, the Cirrus 40/2 includes an internal fan that ensures uniform heat distribution, which is essential to avoid localized hotspots and maintain a stable and homogeneous temperature within the methacrylate chamber. Its nominal 24 V operation aligns with the system's low-voltage electrical design, enhancing safety in a laboratory environment. The modular form factor and lightweight construction allow for easy integration, while its independent fan control circuit provides flexibility to adjust airflow as needed without interfering with the heating logic. Its pre-wired configuration, DIN clip mounting, and IP20 protection rating contribute to a safe and rapid installation.

Similarly to the heating resistors, both units have been electrically prepared through soldering, even though their power and ground supply have not been connected, to allow them to be independent from each other in case one needs to remain *on* and the other *off* in a given scenario. terminals and powered via a relay controlled by the Arduino Uno. As in the previous heating elements, once the system is connected, the microcontroller receives real-time data from TSIC 506F digital temperature sensors within the chamber and activates or deactivates the fan-heaters accordingly, ensuring that the system only operates when needed, maintaining a precise and stable temperature.

Parameter	**Specification**
Heating Power	125–230 W (nominal at 24 V / 100–240 V AC)
Fan Airflow	12.4 m³/h
Operating Voltage	12–24 V (fan); 100–240 V (heater)
Rated Fan Current	0.06 A
Dimensions (L × W × H)	42 mm × 42 mm × 107 mm
Weight	0.260–0.275 kg
Protection Rating	IP20
Mounting Options	DIN rail clip, optional finger guards
Cable Length	600 mm
Control Method	External relay, Arduino-based temperature regulation

Table 2. Technical specifications of the DBK Cirrus 40/2, highlighting its voltage range, temperature control capabilities, and structural features relevant to controlled thermal environments.

Relay-induced Control of the Heating Elements

A relay is an electromechanical switch that allows a low-power electrical signal to control a higher-power circuit safely and efficiently. It consists of a coil that, when energized, generates a magnetic field to move an internal switch, changing the connection between terminals. The key terminals are:

- COM (Common): The moving contact switches between the normally open and closed contacts.
- NO (Normally Open): This contact remains open when the coil is de-energized and closes (connects to COM) when the coil is energized.
- NC (Normally Closed): This contact remains closed (connected to COM) when the coil is de-energized and opens when the coil is energized.

In the initial design, individual SRD-05VDC-SL-C [28] relays were used to control each heating element separately, making a total of 3 relays; one for each heating fan and another for the resistors. This allowed precise on/off switching of each element based on temperature readings from sensors inside the chamber, controlled by the Arduino, however, this approach presented some practical drawbacks, as the need for three separate relays increased the complexity of wiring and physical space requirements, complicated the assembly and maintenance due to additional connections and the overall system footprint was larger, reducing compactness and ease of integration.

A 4-relay module [29] was adopted to overcome these limitations, integrating four SRD-type relays into a single compact board compatible with Arduino digital outputs. This 4-realay module improved space efficiency, simplified wiring considerably (centralizing relay control and power connections, improved cable management, and reducing potential errors), and enabled independent switching for each one of the heating elements.

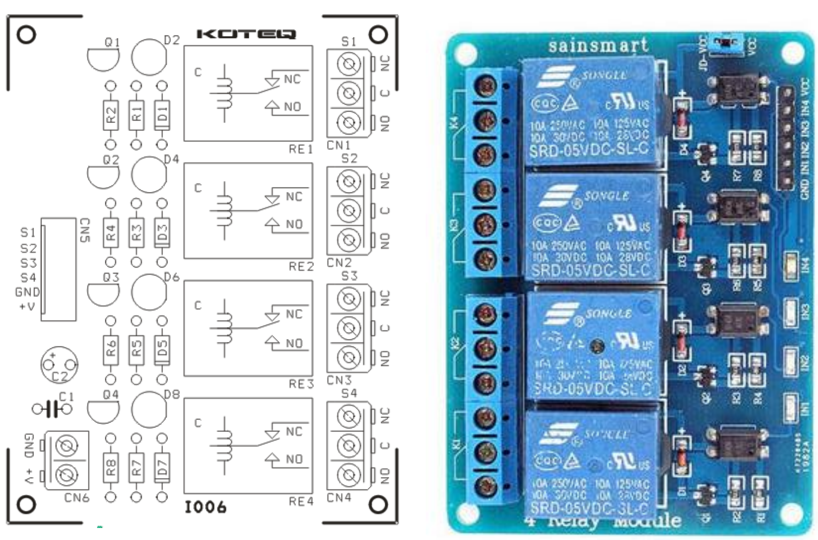

Figure 6.- Electrical diagram and image of the 4-relay module [29] integrated in the system

The heating and ventilation system is controlled by four relays (K1 to K4), each serving a specific function and wired to allow independent control of fans and heating elements, having the following configuration:

1. Relay K4 controls the first heating fan. Its coil is driven by Arduino digital output pin 4. The relay's COM terminal is connected directly to the 24 V power supply. In contrast, the NO (Normally Open) terminal connects to the power input of the internal heating resistor of the first fan. When K4 is activated, it completes the circuit, supplying 24 V to the fan's heating element.

2. Relay K3 controls the second heating fan's resistor. Its coil is driven by Arduino digital output pin 5. It is powered from the COM terminal of K4, effectively sharing the 24 V supply line, and its ground is connected to the 24 V power source. The NO terminal of K3 connects to the heating resistor input of the second fan, enabling independent switching of this element.

3. Relay K2 controls the heating resistors' standard power line at 12 V. Its coil is driven by Arduino digital output pin 6. Its COM terminal connects directly to the 12 V power supply, and the NO terminal connects to the standard input feeding the heating resistors. When K2 is energized, it powers the resistors that generate heat.

4. Relay K1 controls the heating fans' fan function (airflow). Its coil is driven by Arduino digital output pin 7. Its COM terminal is powered from the COM terminal of K2, receiving 12 V, and its NO terminal connects to the power input lines of the fans themselves. The activation of K1 energizes the fans and enables air circulation.

This relay configuration allows the 24 V power supply to feed each fan's heating resistor independently through K3 and K4. In comparison, the 12 V supply powers both the heating resistors (via K2) and the fans' motor function (via K1), whose grounds are connected to the common ground terminal of the 12 V power supply, ensuring a shared reference for the control system, providing independent and precise control of each heating and ventilation element and enabling flexible thermal regulation within the chamber based on sensor feedback and Arduino logic.

5.1.3 Temperature sensors: TMP36 and TSIC 506F

Initially, the temperature monitoring system was designed using the TMP36 analog temperature sensor, which was also employed in the first experimental trials. The TMP36 produces an analog voltage output proportional to the measured temperature. Specifically, it outputs 750 mV at 25°C, with a linear scale factor of 10 mV/°C and an offset of 500 mV at 0°C. This simplicity allows direct temperature reading via an analog-to-digital converter (ADC) on microcontrollers such as the Arduino Uno.

Despite its ease of use and affordability, the TMP36 has certain limitations. As an analog sensor, its output is susceptible to electrical noise and ADC resolution constraints, which can reduce measurement accuracy and stability. Typically, it provides an accuracy of approximately ±2°C, which may be insufficient for high-precision applications.

To address these limitations, the system was upgraded to incorporate three TSIC 506F temperature sensors, a digital temperature sensor that communicates via the ZACWire protocol. The TSIC 506F is factory-calibrated, delivering high precision measurements with an accuracy of ±0.1°C within the critical temperature range of +5°C to +45°C. It operates at low power consumption (around 30 μA at 3.3 V), minimizing self-heating effects that could otherwise distort readings.

Unlike the TMP36, the TSIC 506F provides temperature data in a digital format, which requires decoding timing signals using precise microcontroller routines. This complexity is offset by significantly improved measurement stability, noise immunity, and long-term reliability.

Feature	**TMP36**	**TSIC 506F**
Output Type	Analog voltage	Digital signal (ZACWire protocol)
Accuracy	±2°C	±0.1°C
Power Consumption	Moderate	Very low
Interface Complexity	Simple ADC reading	Requires timing decoding
Noise Immunity	Susceptible to electrical noise	High immunity
Temperature Range	–40°C to +125°C	–10°C to +60°C
Calibration	Factory calibrated, but less precise	Factory calibrated with high precision

Table 3.- Comparison of key features between the TMP36 analog temperature sensor and the TSIC 506F digital temperature sensor.

Regarding TSIC 506F connections with Arduino Uno, its connections are straightforward; the sensors' digital signal pin is connected to one of the microcontroller's digital input slots, while the other two pins ($V,_{cc+}$ and GND) are connected via protoboard to the 5V supply and ground slots Arduino supplies.

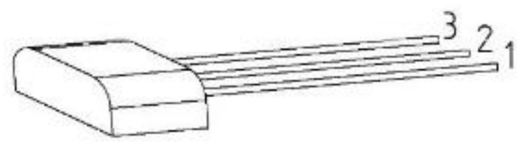

Figure 7.- TSIC 50GF scheme, where: 1. GND, 2. Digital Signal, 3. Vcc (3V to 5.5V). Retrieved from TSIC 50F datasheet [23]

5.1.4 Arduino Uno and Protoboard configuration

The Arduino Uno is powered by a USB from the computer running the control software. Its digital and power pins are configured to manage temperature sensing and actuator control, with connections distributed through a central breadboard to ensure organized and reliable wiring.

· Digital inputs: Pins 2, 3, and 8 are used to read data from three TSIC 506F digital temperature sensors, which provide high-precision temperature measurements for thermal regulation inside the chamber.

· Digital outputs:

1. Pin 4 controls the relay associated with the first heating fan resistor.
2. Pin 5 controls the relay for the second heating fan resistor.
3. Pin 6 controls the relay powering the standard heating resistors.
4. Pin 7 controls the relay that activates the fan function of the heating fans.

· Power distribution: The Arduino's 5V output pin is connected to the main 5V rail of the breadboard, supplying power to components that require a regulated logic-level voltage.

· The GND pin is connected to the ground rail of the breadboard, providing a standard ground reference for all digital components and sensors.

Regarding the protoboard configuration, the breadboard's red and blue power rails are supplied with 5V and GND from the Arduino Uno, respectively, as previously explained. These rails also serve as the power source for the three TSIC 506F temperature sensors, drawing their power (Vcc) and ground (GND) connections from these lines.

Initially, the 4-channel relay module was powered using the same 5V and GND lines from the Arduino. However, experimental testing revealed that as the system approached the programmed target temperature, the frequent switching on and off the relays caused sudden changes in current demand. This transient load exceeded the Arduino's electrical capabilities and compromised the temperature sensors' stability.

This issue is known as voltage sag [30] or power supply brown-out, a phenomenon where a sudden increase in current draw causes a temporary voltage drop, especially in systems with limited current supply capacity like microcontrollers. When the relays activate, their coils briefly demand a relatively high inrush current, which can cause the supply voltage to dip below the minimum operating voltage of sensitive components such as the TSIC sensors. As a result, the sensors produce erratic readings, sometimes fluctuating by several degrees (both positively and negatively). This causes the system to continuously toggle the relays in a feedback loop, preventing the system from stabilizing.

To address this problem, which manifested as noisy sensor signals and temperature readings with step-like fluctuations, a separate 5V power supply was introduced exclusively for the relay module. This external power source decouples the relay module's power requirements from the Arduino and the sensors, ensuring voltage stability for all components.

The positive terminal of this external 5V power supply is connected directly to a separate rail on the breadboard, which is linked to the VCC pin of the relay module. Meanwhile, the GND of the external 5V supply is connected to the common ground shared by the Arduino and the sensors, ensuring a unified reference voltage for the entire system. This approach effectively isolates the power-hungry relay module from the more sensitive logic and sensing components, resulting in stable and reliable temperature control within the experimental chamber.

5.1.5 Electrical configuration

The electrical configuration of the temperature control and ventilation system was modeled and simulated using LTspice® [31], a widely used circuit simulation tool developed by Analog Devices. The simulation environment was designed to replicate the functional behavior of the real system by incorporating representative voltage sources, switching logic, heating elements, and ventilators.

The schematic includes the three DC voltage sources (5 V, 12 V, and 24 V), corresponding to the control logic and power requirements of the system components, as well as the four switches (SW) controlled via relay drivers (K1 to K4), that simulate the digital output behavior of the microcontroller, allowing selective activation of the heating and ventilation circuits.

The heating system is represented by two resistive elements (*Rheat*), each with a value of 30 Ω, modeling the PTC-type heating resistors used in the physical chamber, whereas the ventilation modules consist of resistive-inductive branches, where *Rmotor* (50 Ω) and *Lmotor* (10 mH) emulate the electrical and transient characteristics of DC fan motors.

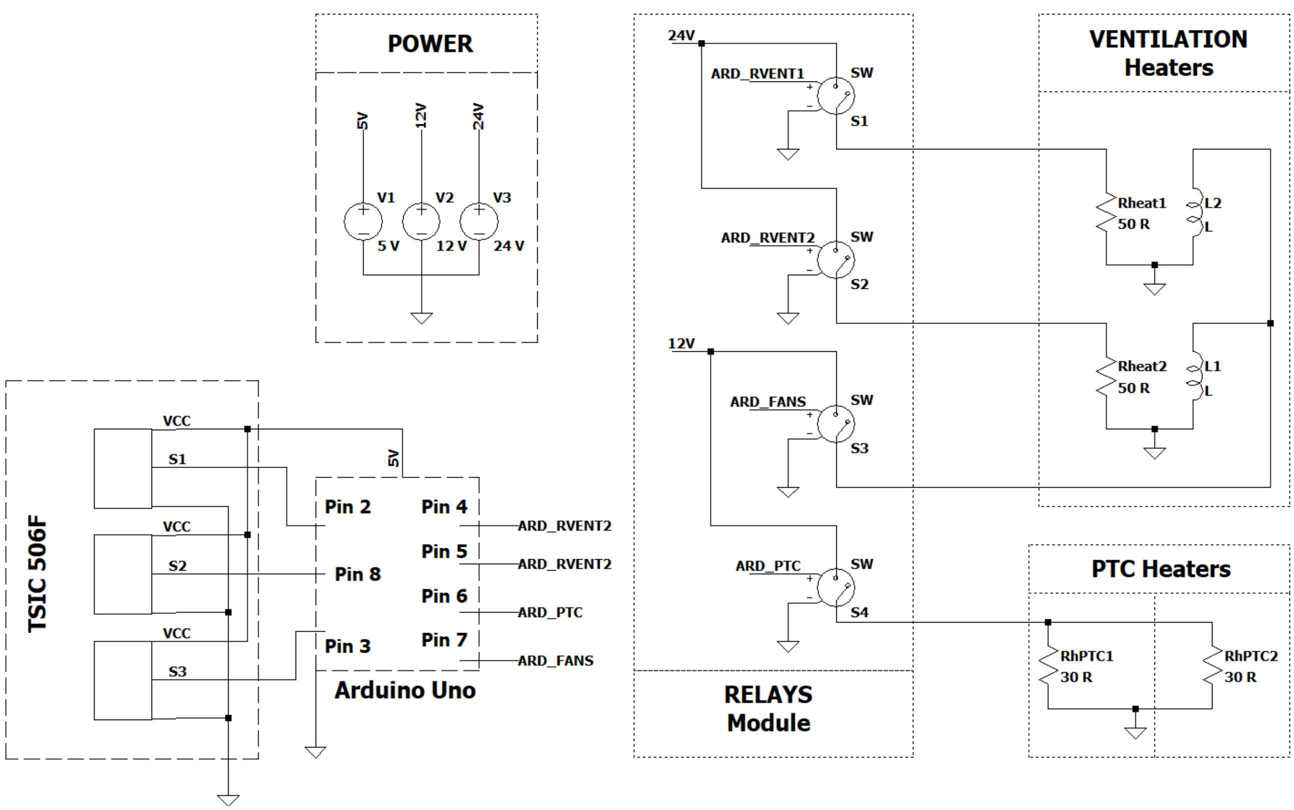

Figure 8.- LTspice [31] schematic of the electrical configuration for thermal and ventilation control.

5.2 Code and Data Visualization

Accurate temperature regulation within the experimental chamber requires precise control logic and reliable real-time system behavior monitoring. A dual-layered software approach was implemented using the Arduino IDE for embedded control and LabVIEW for data visualization. Arduino handles direct sensor readings and actuator control, while LabVIEW provides a graphical interface to display temperature trends and system status.

5.2.1 Arduino Code

The control system implemented in this project [see Annex 1] is based on an Arduino Uno microcontroller, responsible for reading temperature values from three digital TSIC 506F sensors and managing the activation of heating and ventilation components via a 4-relay module. The code developed for this purpose was written in the Arduino IDE using the TSIC library to decode temperature data transmitted via the ZACWire protocol. Each sensor is connected to a dedicated digital pin (2, 3, and 8), and the Arduino reads their temperature values every 2 seconds. These values are converted into Celsius and averaged to obtain a representative temperature of the environment inside the chamber. The resulting temperatures are sent via the serial interface in a comma-separated format, allowing real-time visualization and logging through LabVIEW or a serial monitoring tool.

Temperature Averaging Mechanism

The averaging mechanism plays a crucial role in ensuring accurate and reliable thermal regulation; instead of relying on a single sensor reading, the system calculates the arithmetic mean of the three individual temperature measurements, which is particularly important in experimental setups where heat may not be perfectly or evenly distributed throughout the chamber such as the one proposed. By averaging multiple readings from spatially separated sensors, the system compensates for local thermal gradients and minimizes the impact of localized overheating or underheating. For example, one sensor near a heating element may report a slightly higher temperature than another placed farther away. Taking only one of these values could result in inaccurate control decisions; therefore, averaging provides a more stable and representative metric of the overall thermal condition, improving control accuracy and biological reliability in experiments involving neural precursors.

```
if (Sensor1.getTemperature(&tempRaw1)) {
tempC1 = Sensor1.calc_Celsius(&tempRaw1);  }
if (Sensor2.getTemperature(&tempRaw2)) {
tempC2 = Sensor2.calc_Celsius(&tempRaw2);  }
if (Sensor3.getTemperature(&tempRaw3)) {
tempC3 = Sensor3.calc_Celsius(&tempRaw3); }
float tempAvg = (tempC1 + tempC2 + tempC3) / 3.0;
```

Control Logic

The control logic is implemented using a simple threshold-based system. If the average temperature falls below 36.0 °C, all heating elements and fans are deactivated to prevent overcooling, and a status LED is activated. If the temperature rises above 37.5 °C-or lies within the target range, relays are activated to maintain the internal temperature.

While this approach provides reliable temperature regulation, it follows a bang-bang control strategy. It only switches components entirely on or off based on discrete thresholds, simplifying implementation and ensuring responsiveness. Despite these strengths, this strategy could potentially lead to oscillatory behavior near the threshold limits, especially in systems with thermal inertia. Therefore, a future improvement for this project could be implementing hysteresis or a proportional-integral-derivative (PID) control algorithm for smoother and more energy-efficient transitions.

```
if (tempAvg < TEMP_MIN) {
        digitalWrite(RELAY_HEATER1, LOW);
        digitalWrite(RELAY_HEATER2, LOW);
        digitalWrite(RELAY_RESISTANCE, LOW);
        digitalWrite(RELAY_FAN, LOW);
        digitalWrite(LED, HIGH);
    } else if (tempAvg > TEMP_MAX) {
        digitalWrite(RELAY_HEATER1, HIGH);
        digitalWrite(RELAY_HEATER2, HIGH);
        digitalWrite(RELAY_RESISTANCE, HIGH);
        digitalWrite(RELAY_FAN, HIGH);
        digitalWrite(LED,LOW );
    } else {
        digitalWrite(RELAY_HEATER1, HIGH);
        digitalWrite(RELAY_HEATER2, HIGH);
        digitalWrite(RELAY_RESISTANCE, HIGH);
        digitalWrite(RELAY_FAN, HIGH);
        digitalWrite(LED, LOW);
```

5.2.2 LabView visualization

To ensure effective monitoring and control of the experimental thermal chamber, a custom graphical interface was developed using LabVIEW™ by National Instruments. This interface allows real-time visualization, data logging, and heating system control based on live temperature readings retrieved from the Arduino microcontroller [see Annex 2].

Graphical User Interface (GUI)

The LabVIEW front panel was designed to provide an intuitive, clear visualization of system behavior. It includes the following key elements:

· Real-Time Temperature Graph: A dynamic chart plots three individual temperature readings (Tem1, Tem2, Tem3) and their computed average (AVG) over time. Each temperature signal is color-coded and updated regularly, offering immediate insight into spatial thermal distribution within the chamber.

· Live Numeric Displays: Each sensor's temperature value and the computed average are displayed numerically in degrees Celsius.

· System Status Indicator: A visual indicator dynamically reflects the thermal control state, heating, or cooling, based on the predefined temperature threshold logic. This indicator helps users confirm whether the system maintains the desired range.

· Manual Control Toggles: Two switch controls allow users to manually activate or deactivate the heating resistor and auxiliary fan units if needed for testing or override.

· Temperature Log Grid: An array of logged temperature values is periodically populated and displayed, representing the stored sensor data simultaneously written to an external .txt file for post-experiment analysis.

· Stop Button: A clearly labeled emergency stop button halts data acquisition and safely disengages all hardware control when pressed.

LabVIEW Block Diagram Logic

The back-end of the system consists of a LabVIEW block diagram that integrates multiple subsystems:

· Serial Communication: Using the VISA interface, LabVIEW continuously reads temperature data transmitted via serial communication from the Arduino. The baud rate and COM port are configurable within the front panel.

· Data Parsing: Incoming serial data, formatted as comma-separated temperature values, is parsed using string manipulation functions and then routed to numerical indicators and the plotting subsystem.

· State Determination: LabVIEW evaluates whether the chamber requires heating or cooling based on the average temperature. This logical decision is visualized using a Boolean LED indicator on the front panel.

· Logging and File Management: Parsed data is logged into a text file at a predefined path. Users can specify the save location manually enabling post-process analysis and experimental reproducibility.

· Heater/Fan Control: Although the Arduino manages actuator control directly in this version, the LabVIEW interface includes manual toggles that could be expanded in future iterations for bidirectional control or advanced feedback.

5.3 Final Result

5.3.1 Chamber Assemble

Once all individual components were tested and optimized, the final step involved assembling the complete system. This included mounting the heating elements, sensors, chamber structure, and electronics together into a single, functional unit. While the integration process was mostly straightforward, the most challenging aspect was cable management and internal wiring arrangement, which required careful planning to avoid interference, ensure clean routing, and maintain both accessibility and thermal insulation. After resolving these layout issues, the system was fully operational and ready for validation.

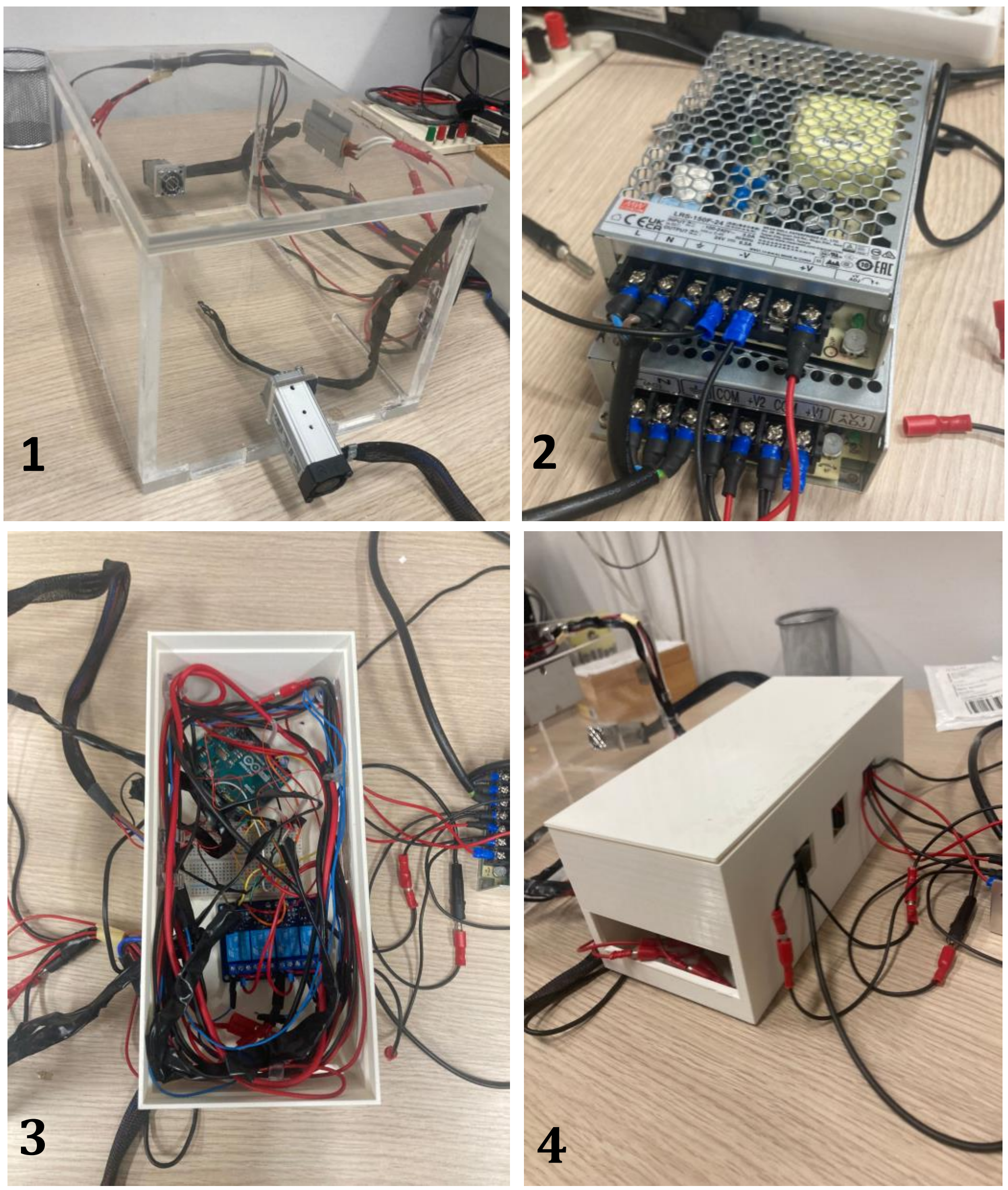

Figure 9.- Images of the final chamber assemble process. 1.- Assemble of the acrylic sheets and heating elements. 2.- Connection with the power supplies. 3 and 4.- Cable management and assemble of the Arduino Uno box.

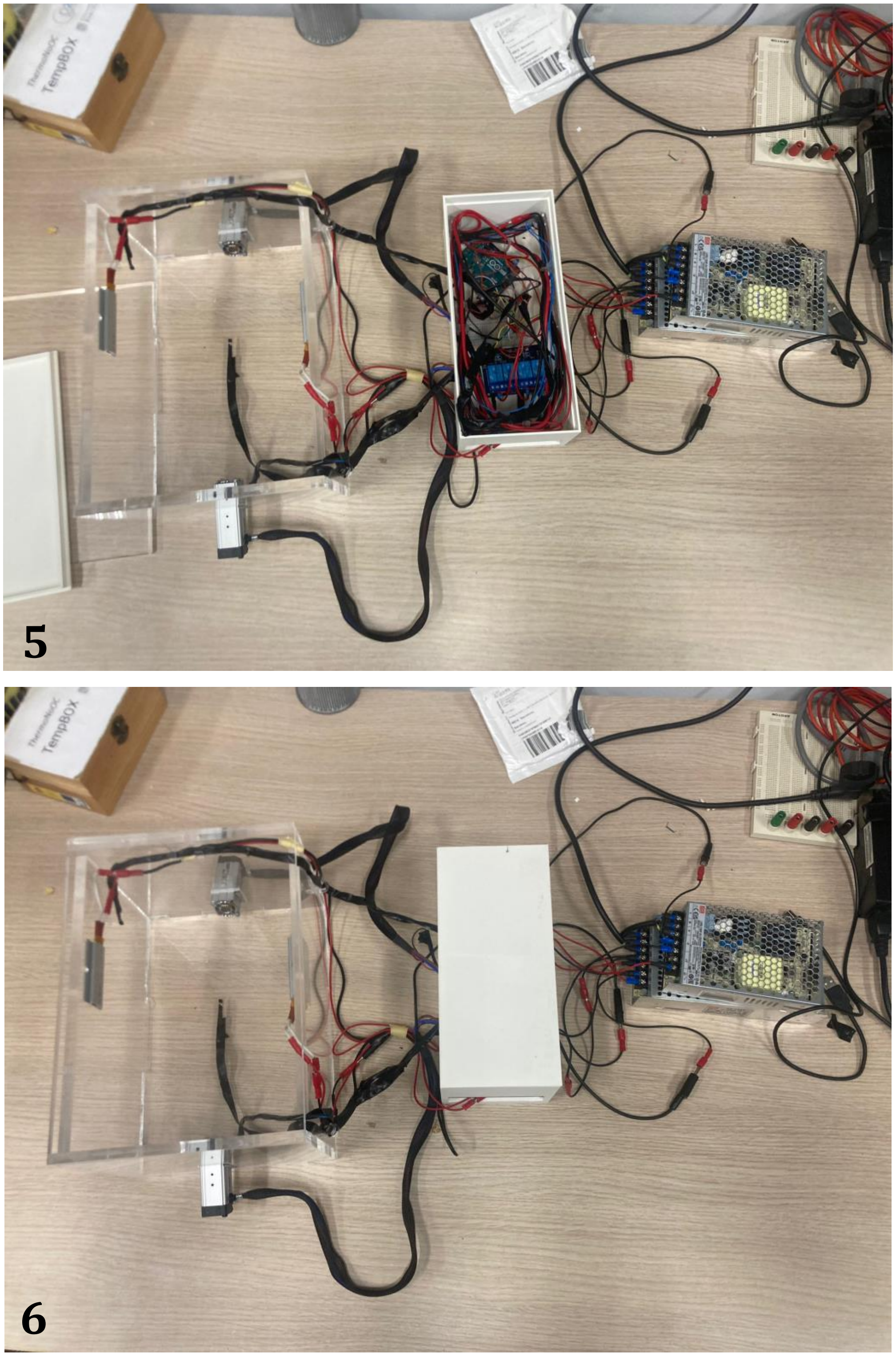

Figure 10.- Image of the final chamber assemble process. 5.-Image of the hole system while functioning showing the Arduino box cable management and the chamber lid off. 6.- Image of the hole system while functioning with all structures closed.

5.3.2 Heat distribution analysis

To validate the performance of the system, a heat distribution study was conducted using a thermal imaging camera RS PRO RS-738S. The goal was to assess whether the chamber effectively maintained a homogeneous temperature and whether the temperature at the center of the chamber — the intended location for the biological samples — matched the readings obtained by the sensors and displayed via LabVIEW.

For this analysis, the thermal camera was positioned vertically above the chamber, capturing top-down images of the internal area. Two sets of thermal images were taken: one with the lid of the chamber on, and another with the lid off. This was done to account for a known limitation of thermal imaging systems, which primarily capture the surface temperature of the materials in their field of view. As a result, the images with the lid on represent the temperature of the upper acrylic surface of the chamber, whereas the images with the lid off provide a more accurate representation of the internal base temperature, closer to the environment directly affecting the biological samples.

To study both scenarios under the same conditions, the system was set to establish an internal temperature of 36 to 37.5 °C, and both images were taken once the internal temperature had stabilized around these desired temperatures according to the LabView readings.

The first image (lid on) [Figure 9] shows the internal surface of the chamber with a clearly defined rectangular region of interest (ROI), marked as R1, over which temperature measurements were taken: the hottest area in the image corresponds to a heating element, reaching a peak temperature of 36.5 °C, while the coldest point registers 29.8 °C near a peripheral, non-heated zone. Within the ROI, the maximum and minimum temperatures are 34.9 °C and 32.9 °C, respectively, with an average of 34.5 °C. The bottom left and top right corners of the rectangle also show slightly cooler temperatures (33.3 °C and 32.9 °C, respectively), indicating the presence of modest thermal gradients, especially diagonally across the region.

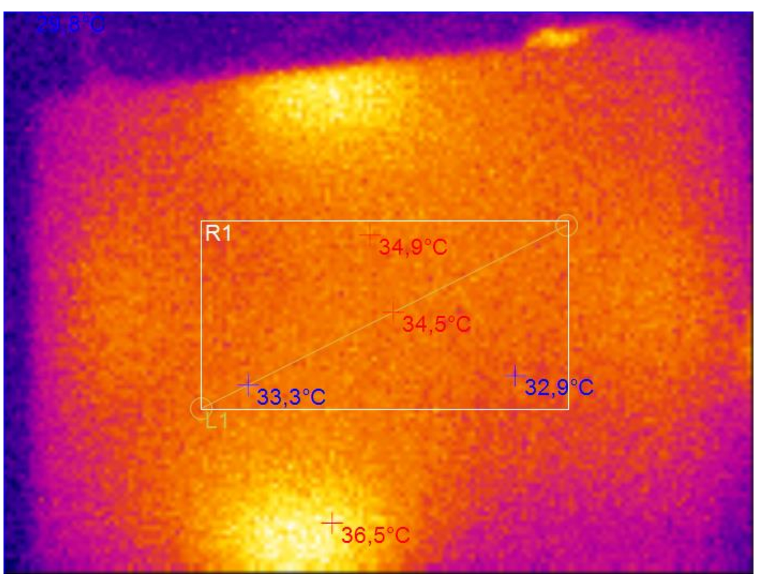

Figure 10.-Top thermal image of the chamber with the lid on taken with RS PRO RS-738S

The second step in validating the thermal uniformity of the experimental chamber was the analysis of spatial and statistical temperature distributions within the defined central region. To do so, the temperature profile along the main diagonal of this region was examined [Figure 10], revealing a fluctuation range between approximately 33.6 °C and 34.6 °C. This spatial variation of ~1 °C indicates the presence of moderate temperature gradients, with a noticeable dip near the midpoint that may correspond to localized cooling or airflow inconsistencies. Such variations suggest that while the overall system achieves a stable mean temperature, it does not exhibit strict isothermal behavior across the chamber's internal surface.

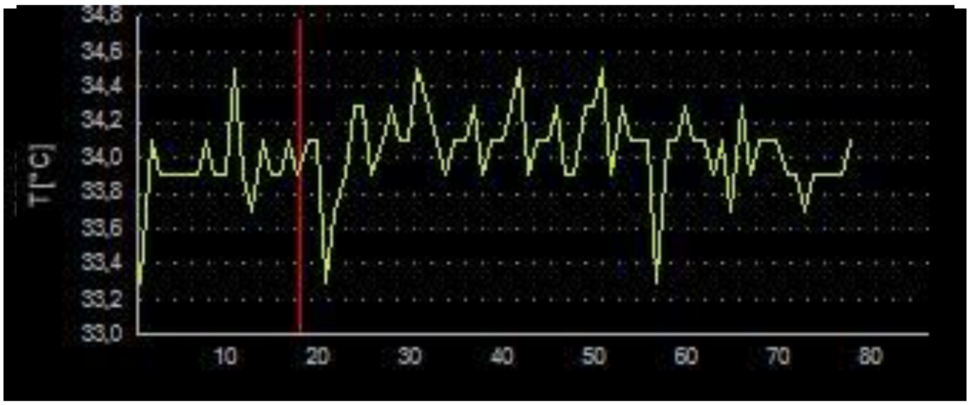

Figure 11.-Top thermal image of the chamber with the lid on taken with RS PRO RS-738S

Complementing this, a histogram-based distribution of temperatures across the entire selected area was also conducted, showing that most temperature readings clustered between 33.7 °C and 34.1 °C, confirming a statistically consistent thermal core. However, the spread observed across a ~1.2 °C range further underscores the presence of small but measurable non-uniformities. These deviations, though minor, may result from factors such as non-homogeneous airflow, surface emissivity differences, or material properties of the chamber components. It should also be remarked that, as mentioned before,

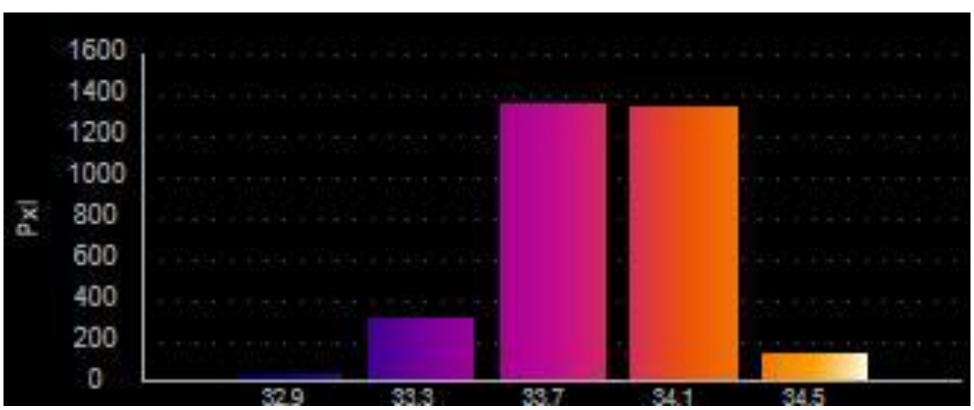

Figure 12.- Histogram of the temperature distribution across the ROI with the lid on

Regarding the second scenario (lid off) [Figure 12], it can be observed that the resulting thermal image reveals a significantly different color scheme compared to the closed-lid scenario, with the central region appearing predominantly in blue and violet tones. This apparent cooling is not due to a reduction in temperature per se but rather to how the thermal camera scales the image's color palette. The color gradient is normalized relative to the hottest object in the frame, which in this case are the exposed heating elements reaching up to 77.9 °C. Consequently, the surrounding air, though it achieved the target temperature of 36 °C, appears artificially cold due to this contrast effect.

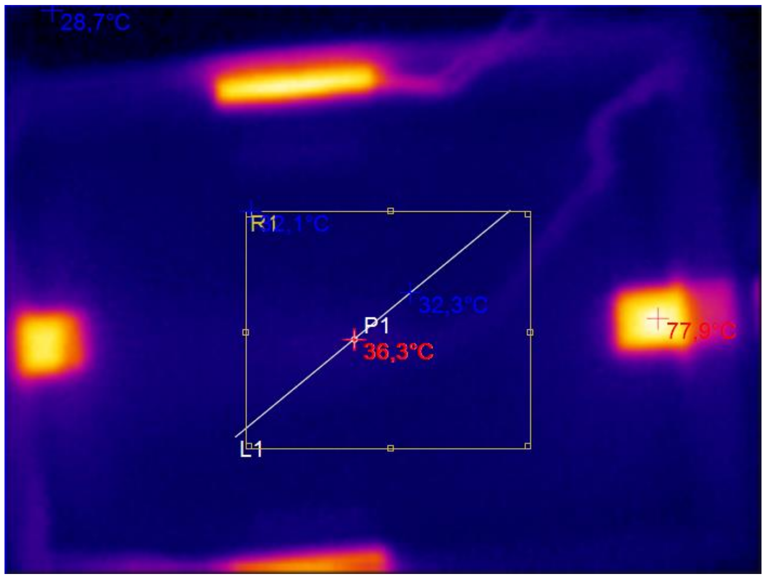

Figure 13.-Top thermal image of the chamber without the lid taken with RS PRO RS-738S

Within the defined region of interest (ROI), the maximum temperature is 32.3 °C, and the minimum is 12.1 °C, with a central measurement (P1) of 36.3 °C. While the average target appears reached near the sensor point, the wide gradient across the ROI demonstrates a notable thermal instability compared to the closed-lid configuration. Additionally, thermal losses at the top (28.7 °C) and corners of the chamber highlight rapid heat dissipation due to unconfined convection and insufficient insulation. The sharp temperature rise near the heating elements also indicates that without a lid, thermal stratification is poorly contained, and localized overheating occurs around the elements.

The temperature distribution graph along the diagonal of the ROI [Figure 13] showed a rising slope peaking around the midpoint, reaching nearly 36 °C, followed by a gradual decline back to 32–33 °C. This behavior confirms the presence of a thermal gradient within the chamber, which is likely influenced by the positioning of the heating elements and air circulation patterns. Despite this gradient, the fact that the central zone approaches 36 °C demonstrates that the system can successfully achieve target temperatures in the region intended for biological experiments.

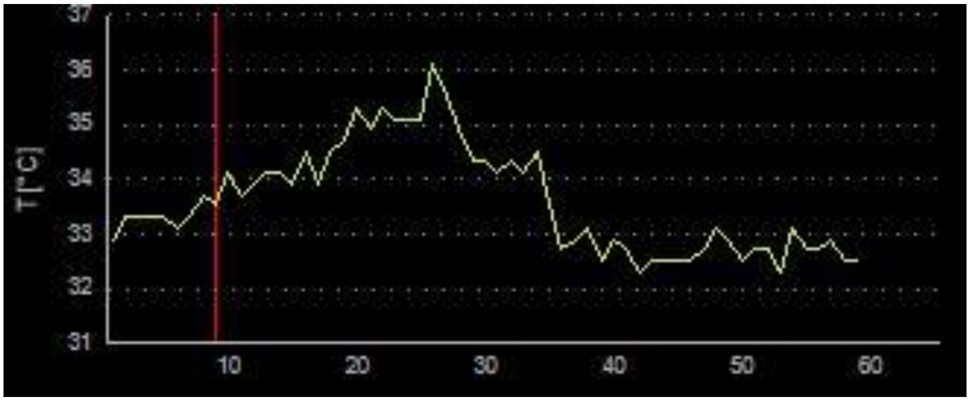

Figure 14.-Top thermal image of the chamber without the lid taken with RS PRO RS-738S

The histogram of pixel temperatures within the ROI [Figure 14] further supported these findings. Most pixels fell between 32.1 °C and 33.8 °C, with a decreasing frequency toward higher temperature ranges. Although the distribution was wider and shifted toward lower values compared to the lid-on condition, this was expected, as the absence of the lid allowed for more convective heat loss and exposed the internal components to ambient air. Importantly, the ability to still reach and maintain a central temperature near 36 °C, aligned with the system's setpoint, validates the effectiveness of the heating and control strategy, even under less insulated conditions.

Overall, the thermal results obtained with the lid off confirm that the temperature-controlled chamber meets its primary design requirements: the central region, where the biological samples are supposed to be placed, reaches the appropriate thermal range, and the values measured by the thermal camera correspond closely to those reported by the system's internal sensors, demonstrating that the chamber can provide a controlled and reproducible environment suitable for temperature-sensitive biological research.

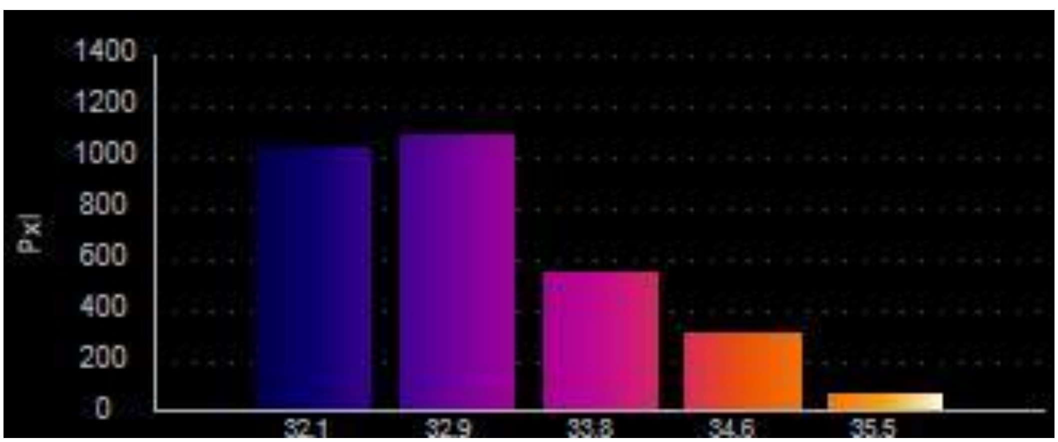

Figure 15.- Histogram of the temperature distribution across the ROI without the lid taken with RS PRO RS-738S

6. Task and time definition: GANTT chart

This section presents a comprehensive breakdown of the project's work structure using a Gantt chart [see Annex 4] and time definition framework. Each activity has been systematically organized into sequential and interdependent tasks, grouped under key project phases such as planning, design, development, and testing. Time allocations are defined in weekly intervals, spanning from February to June 2025.

Task ID	Task Name	Start Week	End Week	Duration (Weeks)
1	Project Planning & Research	1	4	4
1.1	Define objectives, literature review	1	2	2
1.2	Analyze current technologies	2	4	3
2	Requirements Analysis	3	5	3
3	Conceptual Design	4	6	3
3.1	Select chamber concept & components	4	5	2
3.2	Preliminary 3D design (SketchUp, FreeCAD)	5	6	2
4	Detailed Design	6	9	4
4.1	Final chamber design and electronics	6	8	3
4.2	Select & spec all hardware	6	7	2
4.3	Draw wiring/electrical schematics	8	9	2
5	Hardware Assembly	8	12	5
5.1	Order and receive components	9	9	1
5.2	Assemble chamber, microcontroller housing	10	11	2
5.3	Wire electronics, soldering	10	11	2
5.4	Subsystem testing (resistors, sensors, relays)	11	12	2

Task ID	Task Name	Start Week	End Week	Duration (Weeks)
6	Software Development	10	15	6
6.1	Develop and test Arduino control code	10	10	1
6.2	Develop LabVIEW visualization	11	12	2
6.3	Power debugging, calibration and adjustments	13	14	2
7	Integration & Testing	15	19	5
7.1	System integration and full tests	16	19	4
7.2	Validate relay/sensor behavior	18	19	2

Table 4.- Table containing the defined project's tasks and their time definition framework

7. Economic feasibility study

To evaluate the economic feasibility of the temperature-controlled chamber system designed for neurovalidation in epileptic treatment, a detailed cost analysis of all major components used in the hardware system has been carried out, taking into account the real purchase prices for each one of the components, providing an accurate financial budget and giving an overview on what are the main costs that should be taken into account when developing this type of projects.

All components used in this project were carefully studied and selected based on an optimal balance between performance requirements and affordability, since the primary goal was to ensure that the system met the technical demands of temperature control and neural precursor monitoring, while maintaining cost-efficiency to keep the overall budget within reasonable limits for an academic research setting.

Component	Quantity	Unit Cost (€)	Total (€)	Notes
Structure & Chamber				
PMMA sheets (Methacrylate, laser-cut)	1 set	132.07	132.07	High-clarity acrylic for chamber
Acrylic adhesive (RS Pro Super Glue)	1	17.00	17.00	Structural bonding
3D Printed Microcontroller Enclosure	1	10.00 (est.)	10.00	Locally printed
Heating System				
PTC Heating Resistors (ΩDBK HPG Series)	2	16.26	32.52	Self-regulating, compact
DBK Cirrus 40/2 Heating Fans	2	71.19	142.38	Integrated heater + airflow
Relay Module (4-channel)	1	11.14	11.14	Arduino-compatible
Temperature Sensors				
TSIC 506F (Digital)	3	25.05	75.15	±0.1 °C accuracy
Electronics & Control				

Component	Quantity	Unit Cost (€)	Total (€)	Notes
Arduino Uno	1	23.44	23.44	ATmega328P
Breadboard, jumpers, terminals	1 set	8.00 (est.)	8.00	Miscellaneous lab supplies
External Power Supply Unit (5V/12V/24V)	1	548.02	548.02	Laboratory-grade, multi-output
Software				
Arduino IDE	-	Free	0.00	Open source
LabVIEW Full License	1 license	1875.00	1875.00	Full research use
Miscellaneous				
Soldering supplies, cables, screws, etc.	-	10.00 (est.)	10.00	General assembly and prototyping
Total Project Cost			**€2893.72**	

Table 5.- Table containing the quantity, individual and global cost of each component and final price to develop this project

By observing Table 5, it is clear to say that the LabView license and the power supply are the most expensive items, representing almost 83.7% of the total cost. Following this reasoning, it can also be claimed that the core system design—including chamber, sensors, heating, and control—is highly cost-effective, since its final cost is just under 485€, following the principle of balance between performance requirements and affordability mentioned earlier.

8. Regulations and Legal Aspects

In the development and implementation of brain-implantable medical devices, strict compliance with regulatory frameworks and ethical guidelines is essential to ensure the safety, efficacy, and ethical integrity of the process. This section outlines the principal regulations and legal requirements that must be considered for a project of this nature to be advanced toward clinical use and commercial deployment.

Within the European Union, any medical device—especially those intended for implantation in the human body—must comply with Regulation (EU) 2017/745 [32] on Medical Devices (MDR). This regulation governs the design, manufacture, clinical evaluation, and post-market surveillance of medical devices, including high-risk devices such as intracranial implants.

A key requirement of the MDR is the execution of successful clinical trials, which must be authorized by an Ethics Committee and a competent national authority. These trials must demonstrate the device's performance and safety in accordance with ethical standards. Furthermore, patients participating in any trial must provide informed consent, meaning they are fully aware of and understand the potential risks, benefits, and implications of the device's use (MDR Article 62 and Annex XV).

In terms of quality and risk management, the following international standards are critical:

ISO 13485:2016 [33] – *Medical devices – Quality management systems – Requirements for regulatory purposes*: This standard specifies the requirements for a comprehensive quality management system (QMS) for the design and manufacture of medical devices. It ensures that medical devices consistently meet customer and regulatory requirements throughout their lifecycle.

ISO 14971:2019 – *Medical devices – Application of risk management to medical devices*: This standard provides a structured framework for identifying hazards, estimating and evaluating associated risks, and implementing risk control measures throughout the device's development and use.

When dealing with patient data, strict adherence to the General Data Protection Regulation (GDPR)—Regulation (EU) 2016/679 [32]—is required to ensure data privacy and protection. Any personal or biometric data collected during trials must be anonymized or pseudonymized, and patients must be informed of how their data will be used, stored, and protected (Articles 5, 6, and 9 of the GDPR).

In the current stage of this project, the device is strictly experimental and intended solely for use in a controlled laboratory setting. As such, it is not subject to clinical, regulatory, or ethical approval requirements applicable to commercial or clinical devices. The materials, components, and methods implemented were selected for feasibility and prototyping purposes, not for clinical safety or biocompatibility.

9. Conclusion and Future Perspectives

The development of the temperature-controlled chamber for neurovalidation presented in this project can be considered a successful outcome both from a functional and engineering perspective since the system fulfilled its main objectives: it maintained biologically relevant temperature ranges with acceptable accuracy, allowed for real-time monitoring using high-precision digital sensors, and integrated a complete hardware-software feedback loop with visualization through LabVIEW. Additionally, it provided an accessible and modular design using cost-effective components, making it suitable for laboratory-scale experimentation involving neural precursor studies.

From a personal and technical standpoint, this project, and the internship that accompanied it, has been a deeply rewarding experience. I am genuinely proud of the results achieved, not only because the system functions as intended but also because it was designed and built entirely from scratch. Throughout the process, I gained valuable hands-on experience in hardware assembly, sensor integration, relay-based control architecture, and LabVIEW interface development—skills I had always hoped to acquire during my degree and which I now feel confident applying in future projects and professional environments.

Despite these achievements, it is also true that several aspects could be improved in future iterations of the prototype to enhance performance, stability, and experimental reproducibility. First, the thermal uniformity inside the chamber could benefit from more efficient air circulation or convection management, and the addition of internal fans with independent speed control or the integration of a laminar airflow system would help minimize localized hot and cold spots, as observed in the thermal analysis.

Secondly, the thermal insulation of the chamber enclosure could be reinforced, particularly around the lid and external interfaces, to reduce energy losses and improve heat retention, by using materials with higher insulation ratings or the use of double-walled acrylic with air gaps, that could significantly enhance stability, especially in long-duration experiments.

The mechanical design of the chamber, while effective and compact, could also be optimized for improved modularity and scalability. Future versions could incorporate quick-access ports for introducing external probes, humidity sensors, or perfusion lines without compromising the enclosure's thermal integrity.

On the software side, although control logic was simple but effective, it could be upgraded to a PID (Proportional–Integral–Derivative) control algorithm to achieve finer thermal stability and energy efficiency, allowing smoother temperature transitions and reduce oscillations around the target setpoint.

Finally, from an experimental point of view, the platform could be extended to include multi-zone thermal control, allowing different regions of the chamber to be maintained at independent setpoints, opening new possibilities that were raised during the planning of this project, such as gradient-based neural studies within a single experiment.

Annex
Annex I: Arduino Control Code.

```
#include "TSIC.h"  // Librería para sensores TSIC

// Pines digitales para sensores TSIC

TSIC Sensor1(2, NO_VCC_PIN, TSIC_50x);  // Sensor 1 en pin
digital 4

TSIC Sensor2(3, NO_VCC_PIN, TSIC_50x);  // Sensor 2 en pin
digital 5

TSIC Sensor3(8, NO_VCC_PIN, TSIC_50x);  // Sensor 2 en pin
digital 5

// Definición de pines

const int LED = 10;

const int BOTON = 2;

const int RELAY_HEATER1 = 4;

const int RELAY_HEATER2 = 5;

const int RELAY_RESISTANCE = 6;

const int RELAY_FAN = 7;

uint16_t tempRaw1 = 0;

uint16_t tempRaw2 = 0;

uint16_t tempRaw3 = 0;

float tempC1 = 0;

float tempC2 = 0;

float tempC3 = 0;

// Definición de variables

const float TEMP_MIN = 36.0;

const float TEMP_MAX = 37.5;

void setup() {

    Serial.begin(9600);

    pinMode(RELAY_HEATER1, OUTPUT);
```

```
    pinMode(RELAY_HEATER2, OUTPUT);
    pinMode(RELAY_RESISTANCE, OUTPUT);
    pinMode(RELAY_FAN, OUTPUT);
    pinMode(LED, OUTPUT);
    digitalWrite(RELAY_HEATER1, LOW);
    digitalWrite(RELAY_HEATER2, LOW);
    digitalWrite(RELAY_RESISTANCE, LOW);
    digitalWrite(RELAY_FAN, LOW);
    digitalWrite(LED, LOW);
}
void loop() {
    if (Sensor1.getTemperature(&tempRaw1)) {
        tempC1 = Sensor1.calc_Celsius(&tempRaw1);
    }
    if (Sensor2.getTemperature(&tempRaw2)) {
        tempC2 = Sensor2.calc_Celsius(&tempRaw2);
    }
    if (Sensor3.getTemperature(&tempRaw3)) {
        tempC3 = Sensor3.calc_Celsius(&tempRaw3);
    }

    // Promedio de temperaturas
    float tempAvg = (tempC1 + tempC2 + tempC3) / 3.0;

  // Enviar temperaturas a LabVIEW
    Serial.print(tempC1);
    Serial.print(",");
```

```
Serial.print(tempC2);
Serial.print(",");
Serial.print(tempC3);
Serial.print(",");
Serial.println(tempAvg);
// Control de temperatura
if (tempAvg < TEMP_MIN) {
    digitalWrite(RELAY_HEATER1, LOW);
    digitalWrite(RELAY_HEATER2, LOW);
    digitalWrite(RELAY_RESISTANCE, LOW);
    digitalWrite(RELAY_FAN, LOW);
    digitalWrite(LED, HIGH);
} else if (tempAvg > TEMP_MAX) {
    digitalWrite(RELAY_HEATER1, HIGH);
    digitalWrite(RELAY_HEATER2, HIGH);
    digitalWrite(RELAY_RESISTANCE, HIGH);
    digitalWrite(RELAY_FAN, HIGH);
    digitalWrite(LED,LOW );
} else {
    digitalWrite(RELAY_HEATER1, HIGH);
    digitalWrite(RELAY_HEATER2, HIGH);
    digitalWrite(RELAY_RESISTANCE, HIGH);
    digitalWrite(RELAY_FAN, HIGH);
    digitalWrite(LED, LOW);
}
delay(2000);  // Esperar 1 segundo
```

Annex 2: LabVIEW Graphical User Interface (GUI) and Block Diagram Logic

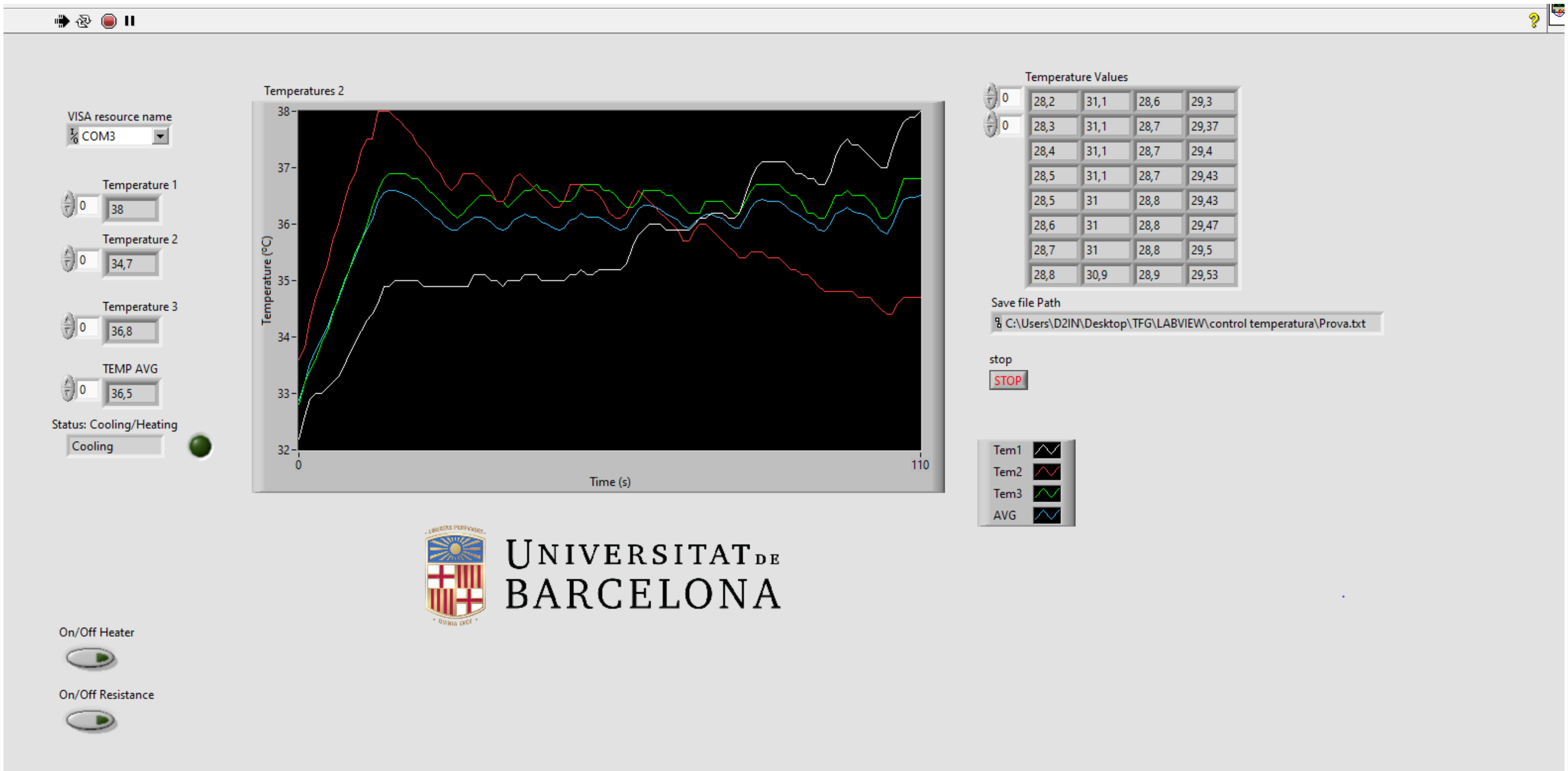

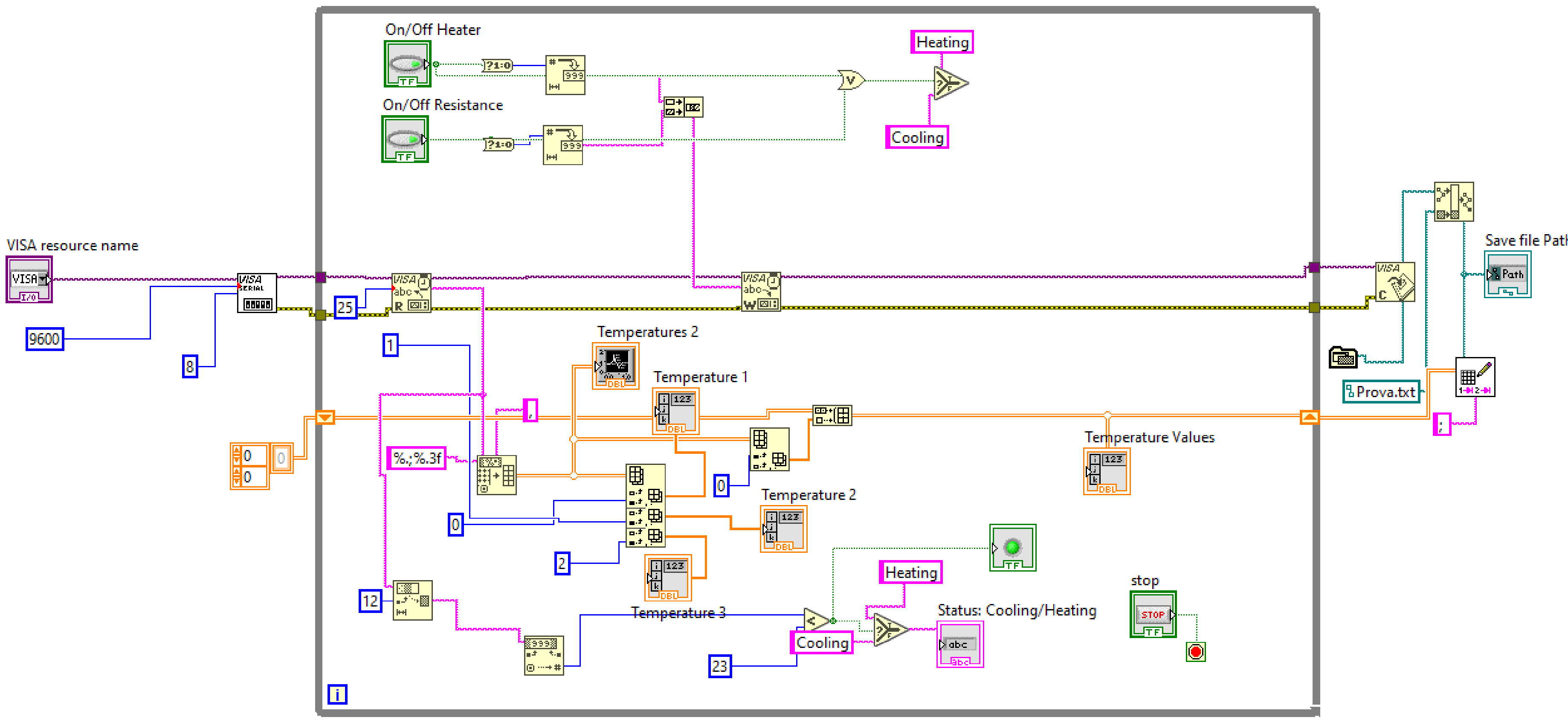

On/Off Heater
On/Off Resistance
Heating
Cooling
VISA resource name
9600
8
25
1
Temperatures 2
Temperature 1
%.;%.3f
0
0
Temperature 2
2
12
Temperature 3
Heating
Cooling
23
Status: Cooling/Heating
stop
Temperature Values
Save file Path
Prova.txt

Annex 3: GANTT Chart of the Project's Tasks and their Time Distribution

Project Planner

All durations are established in weeks, from February 2025 to June 2025.

Period Highlight: 60

Plan Duration | Actual Start | % Complete | Actual (beyond plan)

ACTIVITY	PLAN START	PLAN DURATION	ACTUAL START	ACTUAL DURATION	PERCENT COMPLETE
1. Project Planning & Research	1	2	1	3	100%
1.1 Define objectives, literature review	1	2	1	2	100%
1.2 Analyze current technologies	2	2	3	2	100%
2. Requirements Analysis	3	2	3	2	100%
3. Conceptual Design	4	2	4	2	100%
3.1 Select chamber concept & components	4	1	4	1	100%
3.2 Preliminary 3D design (SketchUp, FreeCAD)	5	1	5	1	100%
4. Detailed Design	6	3	6	3	100%
4.1 Final chamber design and electronics	6	2	6	2	100%
4.2 Select & spec all hardware	6	1	6	1	100%
4.3 Draw wiring/electrical schematics	8	1	8	1	100%
5. Hardware Assembly	8	4	9	4	100%
5.1 Order and receive components	9	1	9	1	100%
5.2 Assemble chamber, microcontroller housing	10	2	10	2	100%
5.3 Wire electronics, soldering	10	2	10	2	100%
5.4 Subsystem testing (resistors, sensors, relays)	11	2	11	2	100%
6. Software Development	10	5	10	5	100%
6.1 Develop and test Arduino control code	10	1	10	1	100%
6.2 Develop LabVIEW visualization	11	2	11	2	100%
6.3 Power debugging, calibration and adjustments	13	2	13	2	100%
7. Integration & Testing	15	4	16	4	100%
7.1 System integration and full tests	16	3	16	4	100%
7.2 Validate relay/sensor behavior	18	2	18	2	100%

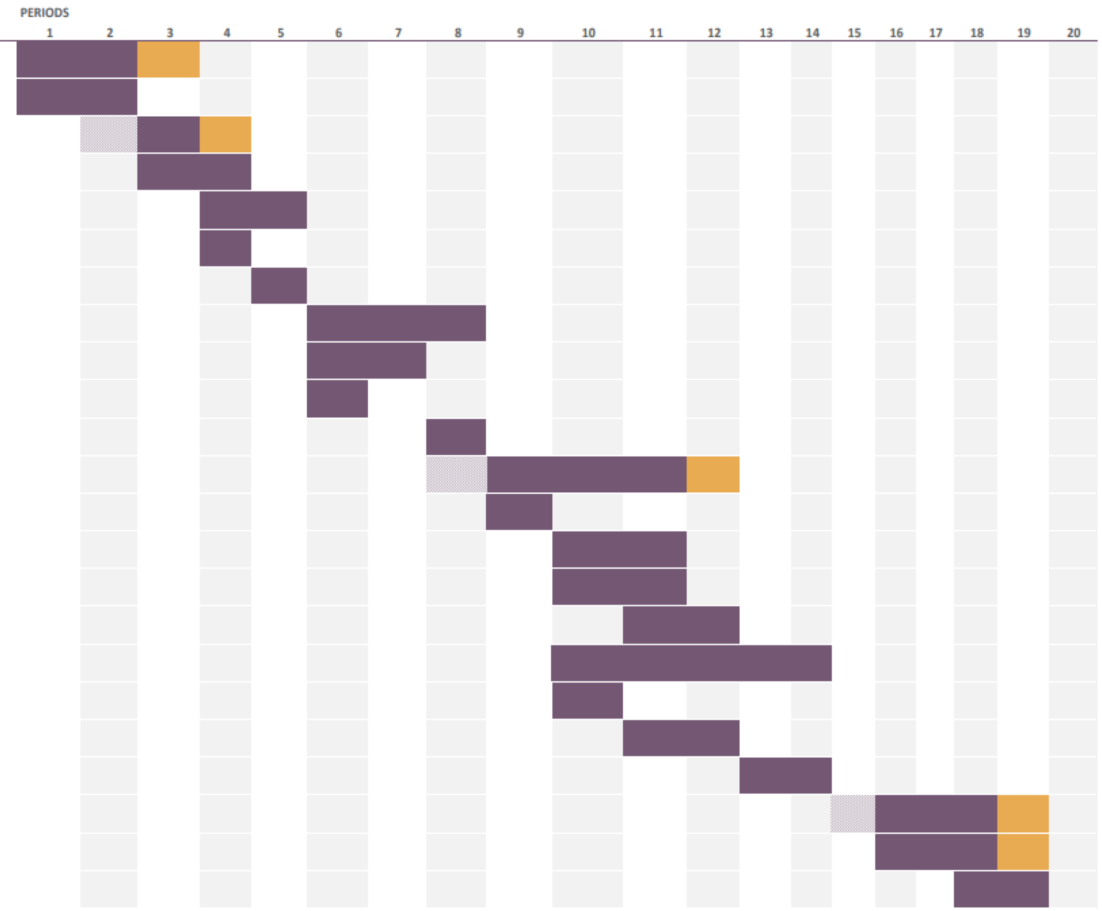

References

[1] Lee, W., Kim, H., Jung, Y., Song, I. U., Chung, Y. A., Yoo, S. S., & Chang, W. S. (2018). Transcranial focused ultrasound stimulation suppresses pentylenetetrazol induced epileptic seizures in vivo. *Brain Stimulation, 11*(4), 689–696.

[2] Jun, J. J., Steinmetz, N. A., Siegle, J. H., Denman, D. J., Bauza, M., Barbarits, B., ... & Harris, T. D. (2017). Fully integrated silicon probes for high-density recording of neural activity. *Nature, 551*(7679), 232–236.

[3] Perucca, E. (2021). The pharmacological treatment of epilepsy: Recent advances and future perspectives. *Acta Epileptologica, 3*, 22. https://doi.org/10.1186/s42494-021-00055-z

[4] Yan, H., Wang, X., Zhang, X., Qiao, L., Gao, R., Ni, D., Shu, W., Xu, C., Ren, L., & Yu, T. (2023). Deep brain stimulation for patients with refractory epilepsy: Nuclei selection and surgical outcome. *Frontiers in Neurology, 14*. https://doi.org/10.3389/fneur.2023.1169105

[5] Nair, D. R., Laxer, K. D., Weber, P. B., et al. (2020). Nine-year prospective efficacy and safety of brain-responsive neurostimulation for focal epilepsy. *Neurology, 95*(9), e1244–e1256. https://doi.org/10.1212/WNL.0000000000009888

[6] Regalado, A. (2024, April 1). Brain-cell transplants are the newest experimental epilepsy treatment. *MIT Technology Review*. Retrieved April 7, 2025, from https://www.technologyreview.com/2024/03/29/1090301/brain-cell-transplants-are-the-newest-experimental-epilepsy-treatment/

[7] ULPGC Library. (2016, November 29). A patch converts your body heat into electricity. Retrieved April 9, 2025, from https://biblioteca.ulpgc.es/blogs/inteling/2016/11/29/un-parche-convierte-el-calor-de-tu-cuerpo-en-electricidad

[8] BBC News Mundo. (2024, April 25). Neuralink by Elon Musk: How telepathy works, the brain chip implanted in a human (and what doubts it raises). Retrieved April 11, 2025, from https://www.bbc.com/mundo/articles/c88np4v0n3zo

[9] Niesvizky-Kogan, I., Bass, M., Goldenholz, S. R., & Goldenholz, D. M. (2022). Focal cooling for drug-resistant epilepsy: A review. *JAMA Neurology, 79*(9), 937–944. https://doi.org/10.1001/jamaneurol.2022.1936

[10] BBC News Mundo. (2024, May 24). Paralyzed man walks again after 12 years thanks to revolutionary brain implant. Retrieved April 13, 2025, from https://www.bbc.com/mundo/noticias-65708310

[11] Serway, R. A., & Jewett, J. W. (2014). *Physics for Scientists and Engineers* (9th ed.). Cengage Learning.

[12] Giancoli, D. C. (2008). *Physics: Principles with Applications* (6th ed.). Pearson Education.

[13] Barrett, S. F., & Pack, D. J. (2012). *Arduino Microcontroller Processing for Everyone! Synthesis Lectures on Digital Circuits and Systems*. Morgan & Claypool Publishers.

[14] Trimble Inc. (n.d.). *SketchUp for Web – Online 3D Modeling | Browser-Based Design*. Retrieved May 1, 2025, from https://www.sketchup.com/es/products/sketchup-for-web?srsltid=AfmBOopdhAC1vunxkDavYaH0j7biChzRUj324YyUrzU4QkiwQ9YLi0Ie

[15] FreeCAD. (n.d.). *Your Parametric 3D Modeler*. Retrieved May 3, 2025, from https://www.freecad.org/index.php?lang=es_ES

[16] Analog Devices. (n.d.). TMP36: Low Voltage Temperature Sensors. Retrieved April 7, 2025, from https://www.analog.com/media/en/technical-documentation/data-sheets/TMP35_36_37.pdf

[17] DBK Enclosures. (n.d.). HPG-2/08-75X35-12-30 | Heating element, length 7.5 mm, width 75 mm, 12 → 30 V AC/DC, 18 W. RS Components. Retrieved April 9, 2025, from https://es.rs-online.com/web/p/elementos-de-calefaccion/7256499

[18] European Union. (2011). Directive 2011/65/EU on the restriction of the use of certain hazardous substances in electrical and electronic equipment (RoHS II). Official Journal of the European Union. Retrieved April 11, 2025, from https://eur-lex.europa.eu/legal-content/EN/TXT/?uri=CELEX:32011L0065

[19] International Electrotechnical Commission (IEC). (2010). IEC 61140: Protection against electric shock – Common aspects for installation and equipment. Retrieved April 13, 2025, from https://webstore.iec.ch/publication/5728

[20] DBK Enclosures. (n.d.). FGC0501.2 Enclosure Heater, 12V DC, 20W Output, 35°C, 72 mm × 27 mm × 27 mm. RS Components. Retrieved April 15, 2025, from https://fi.rsdelivers.com/en/product/dbk-enclosures/fgc05012/dbk-enclosures-enclosure-heater-12v-dc-20w-output/4152931

[21] DBK Enclosures. (n.d.). FGC1507.2 Enclosure Heater, 100–240 V AC, 230 W Output, 120°C, 107 mm × 42 mm × 42 mm. RS Components. Retrieved April 17, 2025, from https://uk.rs-online.com/web/p/enclosure-heaters/4152981

[22] Innovative Sensor Technology IST AG. (2023). TSic 506F/503F/501F Temperature Sensor IC: For a fully calibrated and very accurate low power temperature measurement (Version 2.4.0). Retrieved April 19, 2025, from https://www.ist-ag.com/sites/default/files/downloads/DTTSic50x_E.pdf

[23] Zentrum Mikroelektronik Dresden AG (ZMD AG), & Innovative Sensor Technology IST AG. (2006). TSic™ Precision Temperature Sensor IC: Technical Notes – ZACwire™ Digital Output (Rev. 2.3). Retrieved April 21, 2025, from

https://www.mikrocontroller.net/attachment/85699/IST_TSic_ZACwire_V2.3_Digital_Output_17-Oct-06.pdf

[24] Arduino. (n.d.). Arduino® Uno Rev3 – Technical Datasheet. Arduino Documentation. Retrieved April 23, 2025, from https://docs.arduino.cc/resources/datasheets/A000066-datasheet.pdf

[25] National Instruments. (n.d.). LabVIEW System Design Software. Retrieved April 25, 2025, from https://www.ni.com/en-us/shop/labview.html

[26] RS Components. (n.d.). *HPG Series PTC heating elements datasheet*. Retrieved May 15, 2025, from https://docs.rs-online.com/4259/A700000007658034.pdf

[27] Underwriters Laboratories. (2021). *UL 3135: Appliance Wiring Material – Silicone rubber insulated wire*. UL Standards. Retrieved May 17, 2025, from https://standardscatalog.ul.com/standards/en/standard_3135

[28] Songle. (n.d.). *SRD-05VDC-SL-C relay datasheet*. Retrieved May 17, 2025, from https://datasheet.lcsc.com/lcsc/2011061125_Songle-SRD-05VDC-SL-C_C103701.pdf

[29] HandsOnTec. (n.d.). *4-Channel relay module datasheet*. Retrieved May 17, 2025, from https://www.handsontec.com/dataspecs/4Ch-relay.pdf

[30] Bollen, M. H. J. (2000). *Understanding power quality problems: Voltage sags and interruptions*. IEEE Press. https://doi.org/10.1109/9780780334557. Retrieved May 23, 2025, from https://ieeexplore.ieee.org/book/5274

[31] Analog Devices. (n.d.). *LTspice® simulator*. Retrieved May 29, 2025, from https://www.analog.com/en/design-center/design-tools-and-calculators/ltspice-simulator.html

[32] European Parliament, & Council of the European Union. (2017). *Regulation (EU) 2017/745 of the European Parliament and of the Council of 5 April 2017 on medical devices, amending Directive 2001/83/EC, Regulation (EC) No 178/2002 and Regulation (EC) No 1223/2009 and repealing Council Directives 90/385/EEC and 93/42/EEC (Medical Device Regulation – MDR)*. *Official Journal of the European Union*. Retrieved June 9, 2025, from https://eur-lex.europa.eu/legal-content/EN/TXT/?uri=CELEX:32017R0745

[33] International Organization for Standardization. (2016). *ISO 13485:2016 – Medical devices – Quality management systems – Requirements for regulatory purposes*. Retrieved June 9, 2025, from https://www.iso.org/standard/59752.html

[34] International Organization for Standardization. (2019). *ISO 14971:2019 – Medical devices – Application of risk management to medical devices*. Retrieved June 9, 2025, from https://www.iso.org/standard/72704.html